

<https://doi.org/10.1038/s43247-025-02253-w>

Offshore wind farms modify coastal food web dynamics by enhancing suspension feeder pathways



Emil De Borger^{1,2}✉, Dick van Oevelen², Ninon Mavraki³, Annelies De Backer⁴, Ulrike Braeckman^{1,5}, Karline Soetaert² & Jan Vanaverbeke^{1,5}

Given the global offshore wind farm (OWF) proliferation, we investigated the impact of OWFs on the marine food web. Using linear inverse modelling (LIM), we compared the OWF food web with two soft-sediment food webs nearby. Novel in situ data on species biomass and their isotopic composition were combined with literature data to construct food webs. Our findings highlight the prominent role of hard-substrate species on turbine foundations as organic material inputs for the food web. Hard substrate species account for approximately 26% of food source uptake from the water column and increase carbon deposition on the surrounding seafloor by ~10%. OWFs facilitate a novel food web with a higher productivity than expected based on standing biomass alone, as a result of numerous interactions between a diverse species community. Our study underscores profound effects of OWFs on marine ecosystems, suggesting the need for further research into their ecological impacts.

The installation of offshore wind farms (OWFs) is considered a pivotal strategy in the transition towards a carbon-neutral energy production. Reaching the targets set by the Paris Agreement requires a global 2000 GW installed capacity of offshore wind by 2050¹, necessitating an annual installation rate of 70–80 GW until then. By 2050, this would result in a worldwide expansion of marine space used for OWFs exceeding 500,000 km²², an area roughly the size of Spain.

The installation of bottom-fixed OWFs in coastal seas comes with substantial changes in the physical environment: the turbines provide new habitat to an environment that originally consisted predominantly of soft sediment and overlying water. Artificial hard substrates in the marine environment expand the available habitat for organisms which require a solid substrate for settlement at some stage in their lifecycle. These hard-substrate species, called epifauna or “fouling fauna” (summarized in Degraer et al. (2020)³) are mainly suspension feeders that filter large volumes of water^{4–6}, noticeably affecting primary productivity^{5,7}. Simulations for the North Sea, for example, have shown decreases in primary production up to 60% within OWFs, depending on the marine setting⁸. Simultaneously, these organisms produce (pseudo-)faeces with relatively high sinking rates, which settle in the vicinity of the turbine, enriching the sediment with organic matter⁹. This additional biomass on the hard substrates attracts a variety of predatorial, symbiotic, and commensal species, including several fish

species^{10–14}, resulting in the development of an additional hard-substrate dependent food web. There are generally observed structural differences in community composition along the depth gradient of a turbine^{15,16}, between turbine and scouring protection layer (SPL) habitat, and between the introduced hard substrate and the original sandy environment^{17,18}. These structural differences are also reflected in distinct trophic niches, where different sub-communities exploit different resources, facilitating the coexistence of a large amount of species¹⁹.

While the qualitative changes that the OWFs will bring to local ecosystem structure are becoming evident, quantitative research on the effects of OWFs on food-web functioning and possible spill-over effects is mostly limited to literature-based simulations of effects of planned OWFs^{20–22}. In addition, there is only limited data-driven research on food-web flows within an OWF and how these differ from the original food web^{20,23}. This study fills this gap by reporting on how the presence of OWFs affects the marine food web, using Linear Inverse Modeling (LIM). LIM is a data assimilation method facilitating the integration of data on biomass, stable isotope signatures and carbon cycling processes (such as respiration) for the purpose of quantifying elemental flows within food webs^{24,25}. LIM is highly useful for quantitatively reconstructing pathways within network structures, making it a powerful tool for bridging the gap between incomplete and uncertain empirical data in natural food webs and the analysis of food web

¹Ghent University, Department of Biology, Marine Biology Research Group, Ghent, Belgium. ²Royal Netherlands Institute of Sea Research (NIOZ), Department of Estuarine and Delta Systems, Yerseke, The Netherlands. ³Wageningen Marine Research, Den Helder, The Netherlands. ⁴Flanders Research Institute for Agriculture, Fisheries and Food (ILVO), ILVO Marine Research, Oostende, Belgium. ⁵Royal Belgian Institute of Natural Sciences, Operational Directorate Natural Environment, Marine Ecology and Management, Brussels, Belgium. ✉e-mail: emil.deborger@ugent.be

structures^{25,26}. A data-driven LIM allows assessing the importance of individual food web species in food webs, transfers of carbon in and out of the food web, and biomass production rates. Essentially, these properties translate to ecosystem functions such as food provisioning and carbon burial, which are all directly underpinned by the interactions between organisms in a food web, and their physical environment.

Network indices calculated based on the quantified food web allow to capture aspects of food web functioning. Total food web activity can be expressed by the Total system throughflow (TST) – the sum of all compartmental C inputs in a food web^{27,28}, whereas Finn's cycling index informs about the carbon cycling capacity within the food web. Indices such as link density (the number of links per compartment), and connectance (the proportion of realized links) relate to the ability of the ecosystem to maintain its structure and function in the face of disturbances, as more connections indicate greater resilience against species loss²⁹.

We investigated the carbon flows in the food web of an OWF in the Southern North Sea (NE Atlantic, Fig. 1A). Using novel, targeted field-measurements supplemented with existing information on food web components, we constructed a food web representative of an offshore wind farm (the combination of a wind turbine, SPL, and surrounding soft sediment habitat Fig. 1B), and two food webs of nearby soft-sediment habitat of either coarse (median grain size: $392 \pm 31 \mu\text{m}$) or fine sand ($173 \pm 2 \mu\text{m}$) (hereafter simply called “Coarse” and “Fine”). In the absence of a true control, the food web of the coarse sediment site reflects a habitat similar to what was originally present on the site where the OWF was constructed. While the fine-sediment habitat, which contains a larger species diversity and a higher organic matter content³⁰ was included to allow for a comparison of the artificially increased richness in the OWF with a more natural diverse soft sediment habitat.

Our two main hypotheses are that (1) the construction of OWFs locally enhances carbon cycling, through the activities of suspension feeders that bring C into the food web that subsequently becomes available to other organisms, and (2) there is a more complex food web (in terms of species diversity, link density and connectance) and a higher C throughput in offshore windfarms due to the mix of hard-substrate and the “original” soft-substrate species, compared to homogenous soft sediment habitats. To test the latter hypothesis, we compared OWF food web complexity with a nearby coarse-sandy habitat, but also with a richer fine-sediment habitat. Additionally we aim to discuss potential benefits for fish in the OWF, based on the food web model output.

We found that the construction of OWFs locally enhances carbon cycling through the activities of suspension feeders on the turbine foundations. These organisms account for approximately 26% of food source uptake from the water column in the OWF food web, and subsequently increases carbon deposition to the surrounding seafloor by about 10%. The hard-substrate fauna also appears to be targeted by several fish species, which adapted their diet in the OWF food web. The OWF food web was more complex than the nearby soft sediment food webs in terms of link density and number of components, but metrics such as connectance and Finn's cycling index showed that the OWF food web was less mature, compared to the other two food webs. This indicates that the food web is still evolving towards a stable equilibrium compared to the other habitats, or that the large amount of species present in low biomass prevent the formation of more stable links.

Results

In the results, we first report the composition of the three different food webs, as these were the result of the data-aggregation procedure including novel field samples. Subsequently, we report on LIM results, for which the species compositions were inputs.

Food web composition and complexity

The food webs differed strongly in their species composition, both in terms of species presence, as well as the biomass with which the species groups occurred (Fig. 2). The OWF food web contained the largest number of species ($n = 120$), compared to the Coarse ($n = 57$) and Fine ($n = 92$) food webs, resulting in 65, 41, and 46 components in the food web models respectively, when including SedOM, watPOM, bacteria, phyto- and zooplankton (Fig. 2, Table S1–S3).

Despite this high number of species, total faunal biomass (benthos + fish) was lowest in the OWF food web ($662.0 \text{ mmol C m}^{-2}$), compared to a more than threefold higher biomass in the Coarse food web ($2047.2 \text{ mmol C m}^{-2}$), and a 23-fold biomass in the Fine food web ($12894.2 \text{ mmol C m}^{-2}$). The difference in biomass between the OWF and Coarse food web was entirely due to *Echinocardium cordatum*, which reached a biomass of $1453.1 \text{ mmol C m}^{-2}$ in Coarse, but only $189.9 \text{ mmol C m}^{-2}$ in the soft sediments of the OWF food web. Fish biomass generally represented only a small amount of total biomass, with similar fish biomass in the Coarse ($4.3 \text{ mmol C m}^{-2}$) and OWF food webs ($4.9 \text{ mmol C m}^{-2}$), and almost triple this biomass in the Fine food web ($12.4 \text{ mmol C m}^{-2}$). In the Coarse and OWF food webs, fish biomass was dominated by Pleuronectiformes (72 and

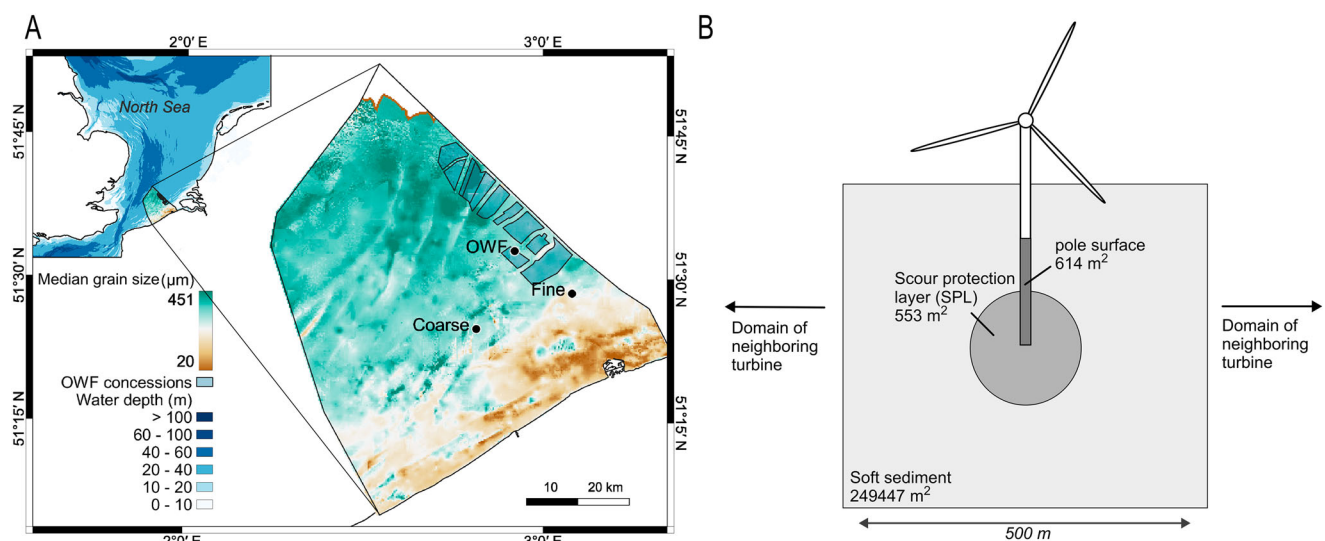


Fig. 1 | Study domain. **A** Location of the three study sites “Coarse” – “Fine” – “OWF” in the Belgian Part of the North Sea (BPNS), showing median grain size in the study area, and bathymetry in the region (inset bathymetry: GEBCO, 2023, grain

size: Verfaillie et al.¹⁰⁸). **B** Structure of the offshore windfarm food web unit (gray surfaces) and indication of the surfaces over which species biomass is standardized to m^2 .

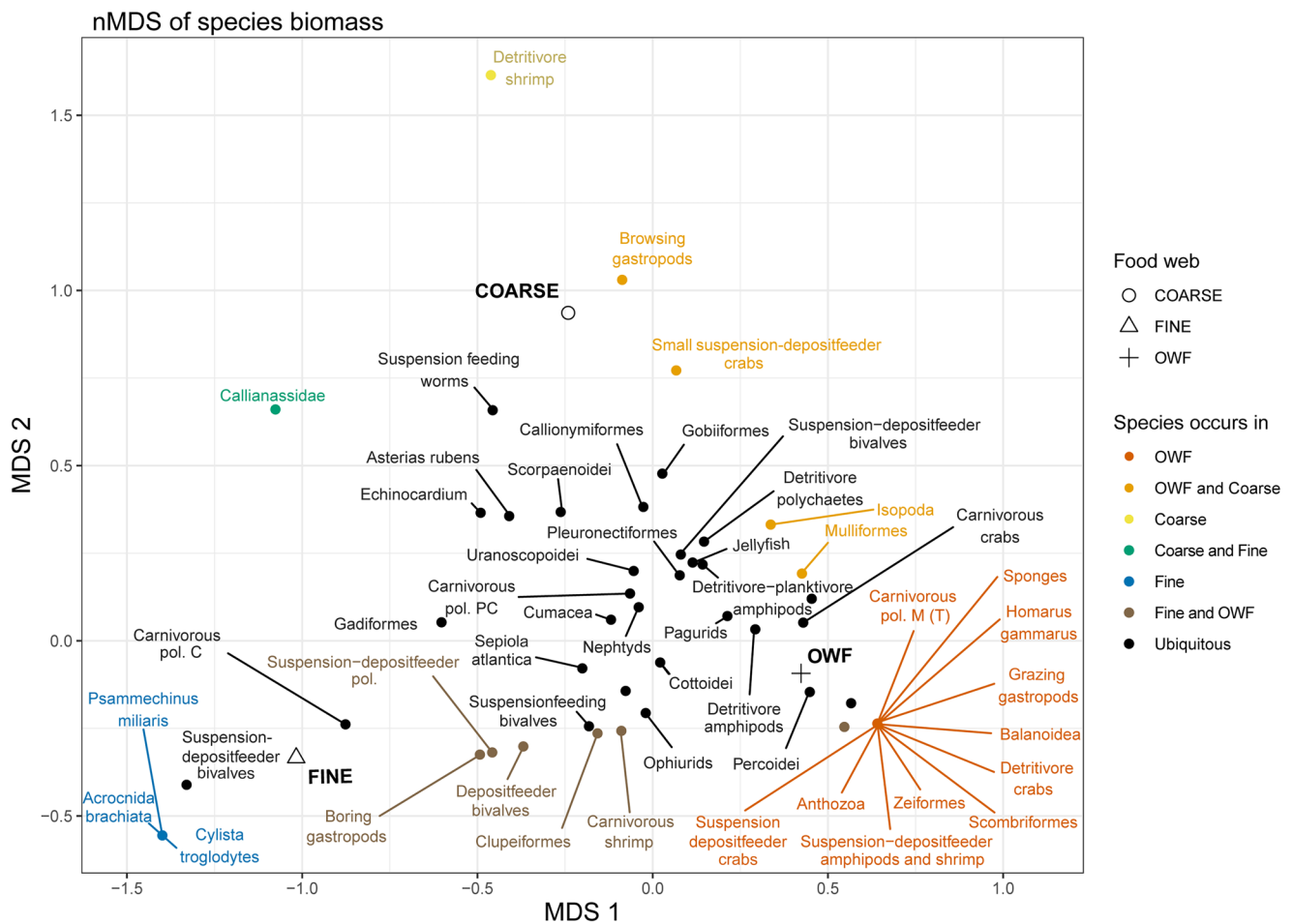


Fig. 2 | Species composition in the different food webs. Non-metric multi-dimensional scaling (nMDS – “Bray-Curtis” dissimilarity) plot of the species groups contained in the Coarse, Fine, and OWF food webs, based on their biomass density (mmol C m^{-2}). Colours indicate in which food web(s) the species groups occur. The

species positions are shown as coloured points, the average position (weighted with component biomass) of the food web is shown as different shapes. Names of several lowest-biomass species are omitted to prevent overlap of labels.

Table 1 | Food web indices

| Index | Full name | units | Coarse | Fine | OWF | % Coarse > Fine | % Coarse > OWF | % Fine > OWF |
|-------|------------------------------|---------------------------------------|--------------------|--------------------|-------------------|-----------------|----------------|--------------|
| TST | Total system throughflow | $\text{mmol C m}^{-2} \text{ d}^{-1}$ | 512.57 ± 1.97 | 698.70 ± 11.47 | 513.88 ± 0.21 | 0.00 | 24.20 | 100.00 |
| Ltot | Total number of links | | 453 ± 0 | 536 ± 0 | 853 ± 0 | 0.00 | 0.00 | 0.00 |
| Lint | Number of internal links | | 374 ± 0 | 447 ± 0 | 726 ± 0 | 0.00 | 0.00 | 0.00 |
| LD | Link density | | 11.05 ± 0 | 11.65 ± 0 | 13.12 ± 0 | 0.00 | 0.00 | 0.00 |
| Tij | Average link weight | $\text{mmol C m}^{-2} \text{ d}^{-1}$ | 1.69 ± 0.004 | 1.73 ± 0.021 | 0.9 ± 0 | 0.00 | 100.00 | 100.00 |
| CI | Connectance | | 0.23 ± 0 | 0.22 ± 0 | 0.17 ± 0 | 100.00 | 100.00 | 100.00 |
| FCI | Revised Finn's cycling index | | 0.0195 ± 0.001 | 0.0277 ± 0.003 | 0.0129 ± 0 | 2.20 | 100.00 | 100.00 |

Calculated food web indices based on 1000 randomly sampled solutions of each food web (mean values \pm SD). Last three columns show results of bootstrapping test: the percentage of solutions where the value of a given index was higher in food web A than higher B, with the contrasts A and B indicated by the column title.

70% respectively), whereas in the Fine food web Pleuronectiformes were second (40.1%) after the Gadiformes (50.9%). Following the higher number of components, the OWF food web had the highest number of links, both total (L_{tot} 853) and internal (L_{int} 726), when compared to the Fine (L_{tot} 536, L_{int} 447) and Coarse (L_{tot} 536, L_{int} 447) food web (Table 1). The connectance index (CI) showed that the proportion of realized links out of all possible links was higher in the Coarse (0.22) and Fine (0.23) food webs, than in the OWF food web (0.17).

Of the 60 species groups, 29 occurred in all three food webs, though not all in a similar biomass (black, Fig. 2). The heart urchin (*Echinocardium cordatum*) dominated biomass in all food webs, representing 75% of the biomass in the Coarse food web, 40% in the Fine food web, and 58% (of soft-sediment biomass) in the OWF food web. *Asterias rubens* was a second important echinoderm, ranging between 7.5 and 14% of the biomass fraction in the studied food webs. There were also pairwise overlaps in composition between the food webs; the OWF food web overlapped with the

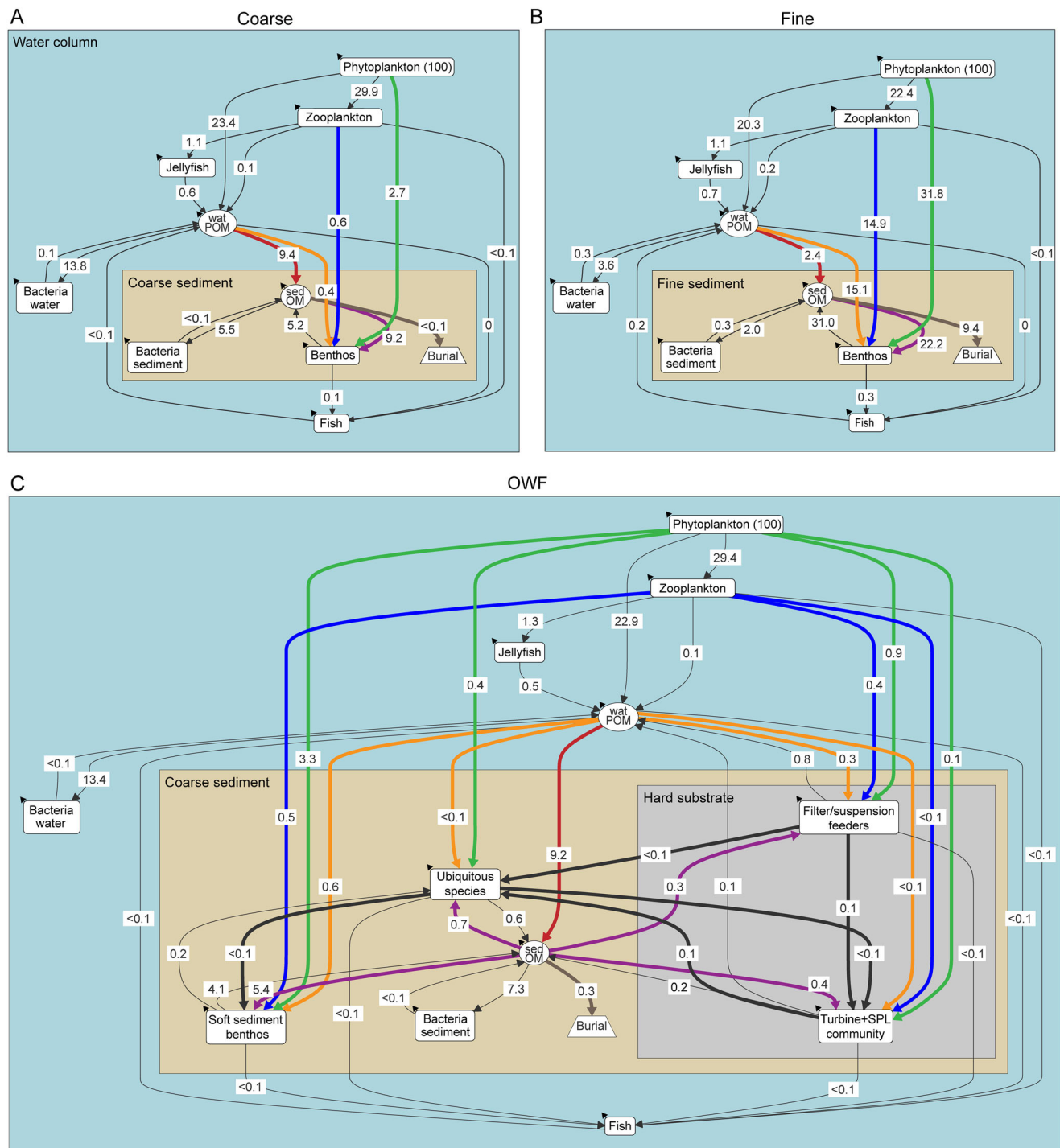


Fig. 3 | Food web carbon flows. Overview of the carbon flows between main (partially aggregated) components of the three food webs represented in percent (%) of the phytoplankton production (net primary production of $250 \text{ mmol C m}^{-2} \text{ d}^{-1}$ indicated by 100 (%)) (A–C). For intercomparison of food webs, similar flows between food webs were coloured green (uptake of phytoplankton by macrofauna), blue (uptake of

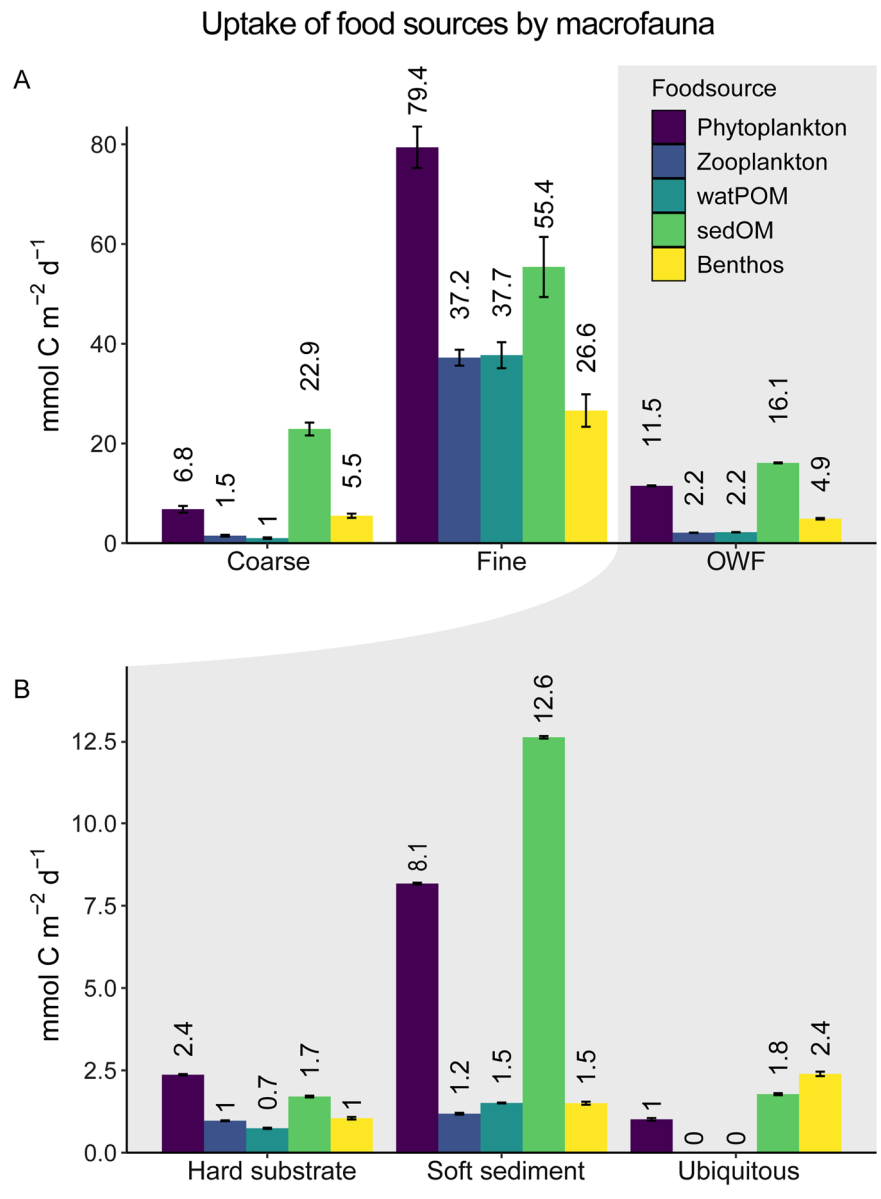
zooplankton by macrofauna), orange (uptake of watPOM by macrofauna), purple (uptake of sedOM by macrofauna), and brown (organic matter deposition on sediment). The small open ended arrows on compartments represent flows of DIC (respiration) and export. Circular boxes represent watPOM and sedOM, rectangular boxes are (aggregated) consumers, and burial is represented by trapezoid boxes.

Coarse (4 groups; Fig. 2: orange points) and Fine (6 groups; Fig. 2: brown points) food webs, whereas the Fine and Coarse food web shared one group (*Callianassidae*, green).

All food webs also contained unique groups, with detritivore shrimp (*Gastrosaccus spinifer*) only found in the Coarse food web, and *Acrocnida brachiata*, *Psammecinus milliaris*, *Cylista troglodytes* and *Epitonium clathratulum* restricted to the Fine food web. Especially the OWF food web contained several species groups occurring on or near

the available hard substrates (24.3% of faunal biomass in this food web, shown by the red names on Fig. 2). This hard-substrate biomass was dominated by the blue mussel *Mytilus edulis* (26.8%), Anthozoans (*Metridium* sp., *Diadumene cincta*, 16.8%), and the amphipod *Jassa herdmanii* (7%). Another large group here are carnivorous crabs, mostly *Cancer pagurus* (and *Necora puber*, *Polybius holsatus*, and *Hemigrapsus* sp.), which represent 30.2% of the macrofaunal biomass living on or near the turbine.

Fig. 4 | Food source uptake per food web. Break-down of uptake flows ($\text{mmol C m}^{-2} \text{d}^{-1}$, y-axis) of different food sources (colours) for (A) Coarse, Fine and OWF food webs, and (B) the subcommunities within the OWF food web: the hard substrate community (turbine + SPL), soft sediment community, and ubiquitous species. Error bars represent SD on 10,000 solutions of the Monte Carlo procedure.



Carbon flows

For each food web, mean values for carbon flows (Table S. 4 for aggregated flow values, and Table S. 5, Table S. 6, Table S. 7 for all flows per food web) and variable values (Table S. 8) were generated through the Markov Chain Monte Carlo (MCMC) procedure. Statements about “lower”, “higher”, or “similar” fluxes and index values are supported by bootstrapping results reported in supplementary materials.

Total carbon throughflow (*TST*) was similar for the Coarse ($512.6 \pm 2.0 \text{ mmol C m}^{-2} \text{d}^{-1}$) and the OWF food web ($513.9 \pm 0.2 \text{ mmol C m}^{-2} \text{d}^{-1}$), and higher in the Fine food web ($698.7 \pm 11.5 \text{ mmol C m}^{-2} \text{d}^{-1}$) (Table 1). The major fluxes in the water column were similar for all food webs. The largest carbon flow in all food webs was primary productivity: the net uptake of dissolved inorganic carbon (DIC) by phytoplankton, which was fixed to $250 \text{ mmol C m}^{-2} \text{d}^{-1}$ (Fig. 3A–C, Table S. 4). In the following section, flows will therefore be expressed as % of this net primary productivity flow (= 100%). In all food webs, about half of the primary production is used in the water column. Zooplankton intake of phytoplankton ranged from 22.4% in the Fine food web, to similar values of 29.4% and 29.9% in the OWF and Coarse food web respectively. A second major fate for phytoplankton is its contribution to the suspended particulate organic matter (watPOM) pool, which is again similar for the

OWF (22.9%) and Coarse (23.4%) food webs, and lower in the Fine food web (20.3%).

Substantial differences were found for fluxes to and from the macrofaunal community, and to and from the detrital organic matter (OM) pools between food webs. Phytoplankton uptake by the macrofaunal community was 31.8% in the Fine food web, but only 2.7% in the Coarse food web, and 4.6% in the OWF food web (1% to hard-substrate community, 3.7% to soft-sediment fauna). The macrofaunal community also consumed zooplankton, with the largest uptake again in the Fine food web (14.9%), 0.6% in the Coarse food web, and 0.9% for the OWF food web (0.4% to hard substrate community, 0.5% to soft sediment community).

Sedimentary OM (sedOM) had two main inputs, deposition of water column POM (Coarse: 9.4%, Fine: 2.4%, OWF: 9.2%), and input from fauna (5.2% in Coarse, 30.6% in Fine, 4.9% in OWF). Following the high macrofaunal biomass in the Fine food web, the flow from benthos to sedOM was 31%, whereas this flow was roughly 1/6th of that in the Coarse (5.2%) and OWF (4.9%) food webs. In turn, the main flows out of the sedOM compartment were respiration by bacteria (Coarse: 5.5%, Fine: 2%, OWF: 7.3%), uptake by macrofauna (Coarse: 9.2%, Fine: 22.2%, OWF: 7.3%), and deep burial, which was highest in the Fine food web (9.5%), and low in the Coarse (< 0.1%) and OWF (0.3%) food webs.

Table 2 | Macrobenthic food uptake

| Food web | Food item | Sublocation | Mean flow \pm SD | 95% CI |
|----------|---------------|---------------|--------------------|-------------|
| Coarse | Phytoplankton | | 6.77 \pm 0.67 | 6.75–6.78 |
| | Zooplankton | | 1.50 \pm 0.18 | 1.49–1.5 |
| | SPOM | | 1.01 \pm 0.15 | 1.01–1.01 |
| | SOM | | 22.90 \pm 1.29 | 22.88–22.93 |
| | Benthos | | 5.53 \pm 0.43 | 5.52–5.54 |
| Fine | Phytoplankton | | 79.40 \pm 4.16 | 79.31–79.47 |
| | Zooplankton | | 37.22 \pm 1.59 | 37.18–37.24 |
| | SPOM | | 37.70 \pm 2.60 | 37.65–37.75 |
| | SOM | | 55.42 \pm 6.03 | 55.30–55.54 |
| | Benthos | | 26.59 \pm 3.25 | 26.52–26.64 |
| OWF | Phytoplankton | Turbine | 2.37 \pm 0.02 | 2.37–2.37 |
| | Zooplankton | | 0.97 \pm 0.01 | 0.97–0.97 |
| | SPOM | | 0.74 \pm 0.02 | 0.74–0.74 |
| | SOM | | 1.70 \pm 0.03 | 1.70–1.70 |
| | Benthos | | 1.05 \pm 0.04 | 1.04–1.05 |
| | Phytoplankton | Soft sediment | 8.17 \pm 0.03 | 8.17–8.17 |
| | Zooplankton | | 1.18 \pm 0.03 | 1.18–1.18 |
| | SPOM | | 1.51 \pm 0.01 | 1.51–1.51 |
| | SOM | | 12.61 \pm 0.04 | 12.61–12.61 |
| | Benthos | | 1.5 \pm 0.04 | 1.50–1.50 |
| | Phytoplankton | Ubiquitous | 1.01 \pm 0.04 | 1.01–1.01 |
| | Zooplankton | | 0 \pm 0 | 0–0 |
| | SPOM | | 0 \pm 0 | 0–0 |
| | SOM | | 1.78 \pm 0.03 | 1.77–1.78 |
| | Benthos | | 2.39 \pm 0.07 | 2.39–2.39 |
| | Phytoplankton | Total | 11.55 \pm 0 | 11.55–11.55 |
| | Zooplankton | | 2.15 \pm 0 | 2.15–2.15 |
| | SPOM | | 2.25 \pm 0 | 2.25–2.25 |
| | SOM | | 16.09 \pm 0 | 16.09–16.09 |
| | Benthos | | 4.94 \pm 0 | 4.94–4.94 |

Total uptake of different food items by macrobenthos in the different food webs (mmol C m⁻² d⁻¹, mean \pm SD).

Macrofauna uptake

There were differences in the proportional macrofaunal food uptake between the food webs (Fig. 4, Table 2, Table S. 4, Table S. 9 for uptake per macrofaunal group). In the coarse sediment food web (Fig. 4A), the total uptake by macrofauna was 37.7 mmol C m⁻² d⁻¹, 2.7% of which was watPOM, 4% zooplankton, 18% phytoplankton, and 60.7% sedOM. The heart urchin (*E. cordatum*) by itself took up the bulk of sedOM (16.3 mmol C m⁻² d⁻¹, Table S. 8), 43% of the total uptake by macrofauna. Uptake of phytoplankton by suspension-deposit feeding bivalves (*Striarca lactea*, *Spisula solida*; 2 mmol C m⁻² d⁻¹) dominated flows for bivalves. The elevated uptake of phytoplankton by crustaceans (4.5 mmol C m⁻² d⁻¹) was caused by suspension deposit feeding crabs, *Pisidia longicornis* and *Thia scutellata*. The total flow between macrofaunal species (carnivory) was 5.9 mmol C m⁻² d⁻¹ (14.7% of uptake).

In the fine sediment, total uptake by macrofauna was 236.3 mmol C m⁻² d⁻¹ – 33.6% phytoplankton, 15.8% zooplankton, 23.5% of sedOM, and 16% of watPOM (Fig. 4A). Again, the uptake of sedOM by *E. cordatum* was the highest single-species uptake (40.5 mmol C m⁻² d⁻¹, Table S. 6). The high phytoplankton uptake was predominantly due to suspension feeding bivalves (69.2 mmol C m⁻² d⁻¹ to *F. fabula*, *A. alba*, *K. bidentata*, *M. balthica*, and *Spisula spp.*), with these species also responsible for more than half of the watPOM uptake in the sediment (23.8 mmol C m⁻² d⁻¹ of

37.7 mmol C m⁻² d⁻¹). Suspension-deposit feeding polychaetes (13.1 mmol C m⁻² d⁻¹), *C. troglodytes* (11 mmol C m⁻² d⁻¹), suspension feeding bivalves (5.1 mmol C m⁻² d⁻¹), and *A. brachiata* (4.9 mmol C m⁻² d⁻¹) dominated zooplankton uptake. The flow between macrofauna species was 26.6 mmol C m⁻² d⁻¹ (11.3% of macrofaunal uptake). Flows to predatory echinoderms (*A. rubens*, *Ophiura spp.*, and *P. miliaris*) represented over two thirds of this flow.

In the OWF food web, the macrofaunal community had a total C uptake of 37 mmol C m⁻² d⁻¹ (Fig. 4A, B), with this uptake predominantly by the soft sediment species (67.6%), followed by the turbine community (Turbine + SPL, 18.5%), and 14% uptake by the ubiquitous species.

Soft sediment species in the OWF (Fig. 4B) mostly fed on phytoplankton (8.2 mmol C m⁻² d⁻¹) and sedOM (12.6 mmol C m⁻² d⁻¹). Again, *E. cordatum* dominated sedOM uptake (8.4 mmol C m⁻² d⁻¹), followed by detritivore polychaetes (1.6 mmol C m⁻² d⁻¹). Phytoplankton uptake was more evenly distributed between different feeding groups such as suspension-deposit feeding bivalves (*Spisula sp.*, 3.2 mmol C m⁻² d⁻¹), pagurids (*P. bernhardus*, *D. pugilator*, 2.6 mmol C m⁻² d⁻¹), and suspension-feeding polychaetes (*L. koreni*, *E. naidina*; 1.4 mmol C m⁻² d⁻¹).

The turbine community (Fig. 4B) mainly consumed phytoplankton (2.4 mmol C m⁻² d⁻¹, driven by *M. edulis*, 2.1 mmol C m⁻² d⁻¹), and sedOM (1.7 mmol C m⁻² d⁻¹) mostly taken up by crustaceans (e.g. crabs: *C. pagurus*, *Hemigrapsus spp.*, *P. holsatus*, *N. puber*; and suspension-deposit feeding amphipods: *J. herdmani*, *P. marina*).

Ubiquitous species (Fig. 4B) were dominated by predatorial-scavenging species (*A. rubens*, carnivorous polychaetes (incl. Nephthyds), and isopoda), as shown by the highest share of uptake of other macrofauna (2.4 mmol C m⁻² d⁻¹), followed by sedOM (1.8 mmol C m⁻² d⁻¹).

The suspension feeders on the turbine were prey to other species on the turbine (0.13 mmol C m⁻² d⁻¹), and in turn the full turbine community was preyed upon by the ubiquitous species (0.2 mmol C m⁻² d⁻¹) (Fig. 3). The ubiquitous species also fed on the soft sediment species (0.45 mmol C m⁻² d⁻¹), while the reverse feeding flow was smaller (0.04 mmol C m⁻² d⁻¹).

Summarized, carbon flows in the Coarse food web sediment were dominated by the uptake of sedOM by *E. cordatum*, making this a detritus-based food web. *E. cordatum* was also strongly present in the Fine food web, but the addition of more suspension feeding groups (bivalves, -polychaetes) generated additional inflows of phyto- and zooplankton, and watPOM, resulting in a more balanced intake of available food sources. In the OWF food web, 68% of C uptake occurred on the soft sediments, dominated by *E. cordatum* feeding on sedOM and suspension feeders feeding on phytoplankton, whereas suspension feeders and scavengers on the turbine / SPL generated additional input of phyto- and zooplankton and sedOM, resulting in total uptake being dominated by phytoplankton and sedOM. Ubiquitous species in this food web consisted mostly of mobile scavengers, capable of feeding on other species both in the soft sediment and the hard substrate.

Fish uptake

In all of the food webs, fluxes from and to the fish were small compared to the macrofaunal component (Fig. 3, flow values in Table S. 10). The Pleuronectiformes by far dominated food uptake in the Coarse and OWF food web (Fig. 5A, C), and closely followed the Gadiformes in the Fine food web (Fig. 5B).

There were testable significant differences between proportional diet compositions of fish species between food webs (Figure S. 1 for proportions visualized), with some general trends as indicated by the PERMANOVA (Table S. 11) and subsequent SIMPER analysis (Table S. 12). We observed a decreased proportion of crustacean prey in the Fine food web compared to the other food webs for several species groups (e.g., Callionymiformes, Carangiformes, Ammodytidae). This was more variable between the Coarse and OWF food web depending on the species: the Gobiiformes and Pleuronectiformes had a higher uptake of crustaceans in the Coarse food web, while higher crustacean uptake in the OWF food web was observed for Carangiformes, Gadiformes and Cottoidei. The uptake of other prey such as

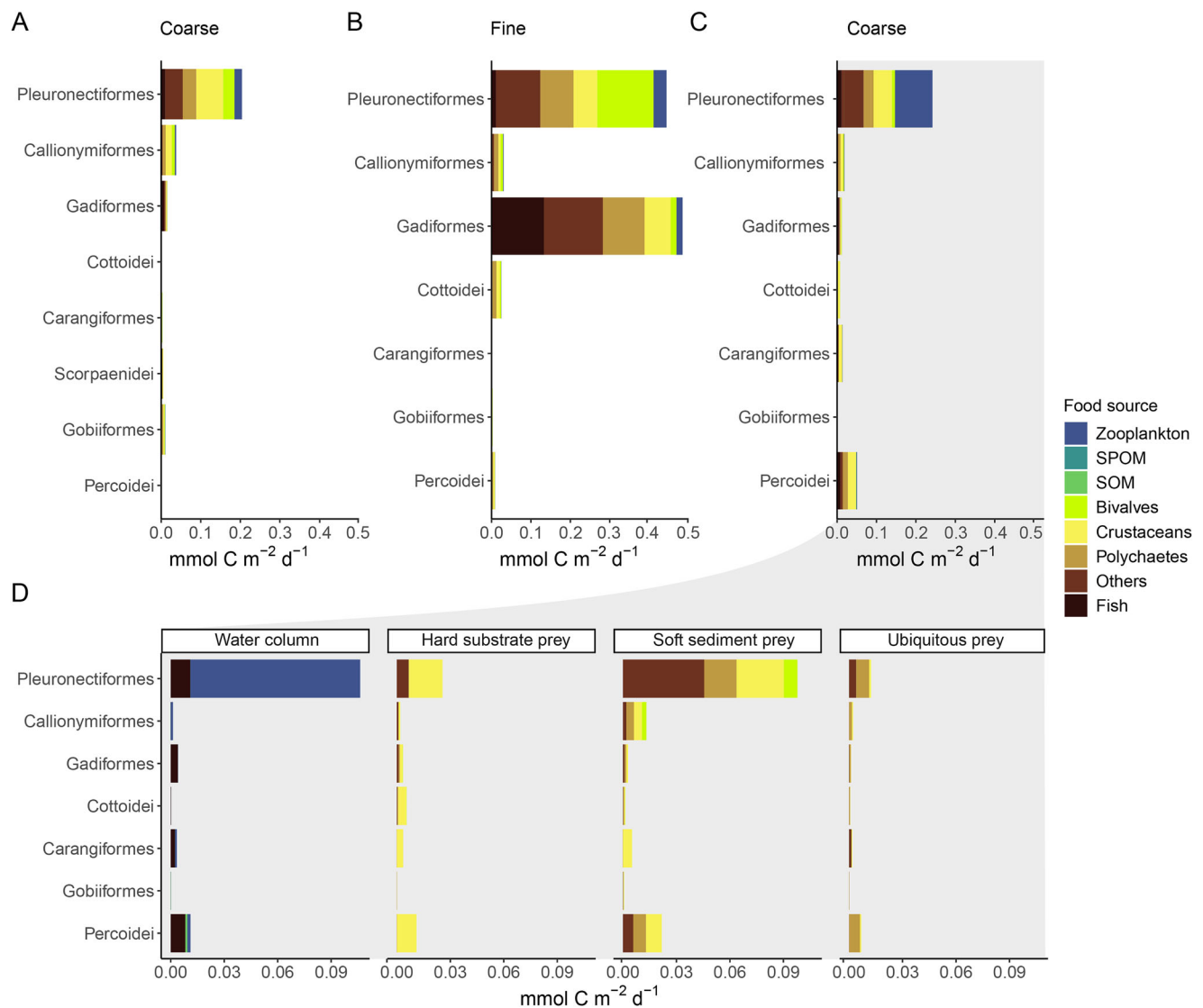


Fig. 5 | Fish feeding preferences. Breakdown of the uptake of different food sources by fish of (A) the Coarse, (B) Fine, and (C) OWF food web (in mmol C m⁻² d⁻¹). In panel (D) the OWF uptake is divided further into general (water column sources),

hard substrate (the turbine – SPL community), soft sediment, and ubiquitous species groups on which fish can feed.

polychaetes, bivalves, and other macrofauna (ophiurids, echinoderms) was higher in the Fine food web than in the other food webs for several fish species. Another trend was that the uptake of fish prey was lower in the OWF food web for several species groups when compared to the Coarse, and Fine food web (e.g., Carangiformes, Scorpaenidae). Especially compared to the coarse food web, five species groups had a significantly lower fish prey uptake in the OWF (Carangiformes, Gadiformes, Percoidei, Scorpaenidae, Pleuronectiformes), whereas compared to the Fine food web three species did (Carangiformes, Gobiiformes, Scorpaenidae). In the OWF food web, Percoidei and Ammodytidae had a higher uptake of fish prey compared to the fine food web.

Looking specifically at the feeding behaviour of fish in the OWF food web, we saw that the hard substrate prey were crustaceans (Fig. 5D), whereas in the surrounding soft-sediment the prey types were more distributed between bivalves, crustaceans, polychaetes, and others (e.g., echinoderms) (Fig. 5D). Also in the OWF food web, most fish species (except for Clupeiformes and the Zeiformes) included Turbine-SPL species into their diet, from low amounts (e.g., Callionymiformes – 10.3%, Gobiiformes – 6.6%, or Scombridae – 8.8%) to the majority of the diet (Cottoidei – 71.7%). For most fish groups in the OWF food web, the soft-sediment fauna remained the majority of their prey intake (Fig. 5D).

Total fish production (the sum of all fish production rates per food web, Table S. 8) was slightly higher in the OWF food web (0.12 ± 0.01 mmol C m⁻² d⁻¹) than the coarse sediment food web (0.11 ± 0.01 mmol C m⁻² d⁻¹), and was highest in the Fine food web (0.32 ± 0.02 mmol C m⁻² d⁻¹).

Carbon outflows

Carbon exports from the three food webs were in the form of export of organic carbon or DIC production from respiration (Table S. 13). Total export (export of phytoplankton, zooplankton, or fauna) was largest in the OWF food web ($71.7 \pm 0.1\%$), closely followed by the Coarse sandy food web ($70.5 \pm 0.8\%$). In the Fine food web, export was considerably smaller ($49.3 \pm 5.4\%$), mostly due to the lower export of phyto- and zooplankton from this food web (Table S. 13). The large benthic component in the Fine sandy food web caused this food web to have the largest respiration ($41.3 \pm 1.4\%$), followed by the Coarse ($29.5 \pm 0.3\%$) and the OWF food web ($28.3 \pm 0.1\%$), which were more similar.

Discussion

In this field data driven study, we quantified the effect of introducing OWFs on soft substrates, with respect to the functioning of the marine food web. The LIM approach was instrumental in this study to describe differences in

food web structure, while simultaneously allowing the estimation of carbon transfer from the base of the food web to the level of fish species. The major modification to the food web upon the introduction of artificial hard substrates into this environment is the additional link between the water column and the seafloor generated by the epifauna on the turbine foundation and SPL. In what follows, we discuss the peculiarities of the OWF food web compared to natural soft substrate food webs, explore potential benefits of OWFs for fish and expand to the regional level of multiple OWFs.

Suspension feeders as the base of the OWF food web

Suspension feeding epifauna occurred in high biomass on the turbines and SPL (15,797 mmol C m⁻² of suspension feeding biomass on hard substrate as compared to 42 mmol C m⁻² of suspension feeders on the OWF sediment), as previously observed in other offshore wind developments^{31,32}. The epifaunal biomass on hard substrates amounted to about 25% to the total macrofaunal biomass in the OWF food web, even though the surface available to hard substrate species represents only 0.5% of the total area of the OWF food web area (1167 m² of turbine + SPL, versus 249,447 m² soft sediment).

This concentration of suspension feeders on the turbine has a prominent effect on the benthic food web in terms of carbon transfer. Species living on the hard substrates were responsible for approximately 26 percent of uptake of water column food-sources – 20.5% of phytoplankton and 45% of zooplankton uptake, due to the increase in filtration capacity. In comparison with the Coarse sandy site, which was dominated by deposit feeders, the increased filtration capacity represented an additional significant input of carbon into the food web of about 14% of carbon uptake by macrofauna (Table 2). In the Coarse food web, uptake of organic matter was dominated by the detritivore *E. cordatum*, resulting in a benthic food web centred around sedimentary organic matter (Fig. 4). *E. cordatum* was also found in sediments adjacent to the wind turbine, though the individuals in these samples were mostly juveniles, and much smaller compared to those in the coarse sand samples (average individual weight of 83 mg C ind⁻¹ versus 1744 mg C ind⁻¹ respectively, Table S. 1, Table S. 3), a consistent observation for the area (Braeckman, pers. comm.). *E. cordatum* is known to be highly sensitive to bottom-disturbing activities such as dredging, which also takes place during the construction of OWFs (seabed preparation, burial of cables). Our observations potentially represent the lengthy recovery process for this slow growing species^{33–35}, as the construction of the OWF was only completed 5–6 years before sampling. When compared to this sedOM-based (Coarse) and sedOM – phytoplankton-based (OWF) food webs, the Fine sandy food web displays a more even mix of available carbon inputs, as a rich community of suspension feeders imports various sources of organic matter (phytoplankton, zooplankton, watPOM, sedOM; Fig. 4) into the sediment.

In the OWF food web, a part of this organic matter input to the sediment community passes through the hard substrate fauna, in the form of faecal pellets and other exudations. In the Coarse and Fine sandy food web, the pelagic carbon is channelled directly to the benthic suspension feeders. From the presented food web analysis, we can estimate the deposition flux of faecal pellets by the turbine community. We have quantified the contribution of epifaunal organisms on the turbine and SPL to the suspended organic matter pool to be around 2 mmol C m⁻² d⁻¹ (where m⁻² denotes the area of the OWF), and 0.6 mmol C m⁻² d⁻¹ directly to the sedimentary organic matter pool. The total deposition flux of OM (watPOM → sedOM) per m⁻² of OWF food web was 22.9 mmol C d⁻¹. Assuming those 2 mmol C m⁻² d⁻¹ to be predominantly in the form of heavy, locally sinking faecal pellets, we estimate that about 8.7% of the OM deposition flux in the OWF food web stems from (pseudo-)faecal pellets (and likely dead organisms). This flux rises to 11.6% if we include the direct contribution of fauna on the SPL to the sedimentary organic matter pool through drop-off (a pathway without passage through the water column). With this contribution of carbon to the sedimentary OM pool by the suspension feeders on the turbine, we confirm our first hypothesis, that the suspension feeders enhance carbon cycling on the scale of the wind farm.

Our estimates of increased deposition fall into the range of previous estimates, acquired from different methodologies. Ivanov et al. 2021³⁶ produced estimates of 2–15% total organic carbon enrichment on distances < 2 km from a monopile, through the use of a hydrodynamic model (including only *M. edulis*). A different modelling study³⁷, using coupled hydrodynamic – dynamic energy budget (DEB) modelling of *M. edulis*, estimated OM deposition to increase by 11–32% in the vicinity (< 40 m) of a turbine foundation, though these estimates are hard to compare with our data as the study took place in very shallow water surrounding smaller turbines. Based on experimentally derived clearance rates combined with arithmetic upscaling, the contribution of *J. herdmanni* to the total deposition flux in offshore wind farms was estimated to be 0.3–0.9%⁵, while in our study *J. herdmanni* contributes between 0.7 and 1% to the depositional flux. As such, available studies so far suggest that the presence of the turbine community results in an “enrichment” effect of about a 10% increase in C deposition on the scale of a wind farm.

Organic carbon burial estimates in the OWF sediments are 80 times higher than those in the Coarse food web (Table S. 4), despite the fact that primary production is the same, and both sediments are permeable (burial rates in Fine sediment were around 30 times higher than in the OWF). Permeable sediments are generally well oxygenated and usually low in OM content^{38,39}, and sedimentation of organic matter (i.e., after a phytoplankton bloom) results in short episodes of intense OM mineralization until almost all OM is recycled³⁹. We suggest that the sustained enrichment in the OWF sediments is due to the continuous supply of OM as faecal pellets (versus episodic after the phytoplankton bloom), and/or linked to certain properties of the deposited faecal pellets such as diminished biogeochemical or physical degradability.

The OWF food web productivity, complexity and stability

Coarse sandy sediments tend to be relatively food scarce, particularly outside of the phytoplankton bloom period, as mineralization of organic matter occurs rapidly due to the high oxygen availability in these sediments^{38,40,41}. A reasonable assumption would be that a consistent 10% increase in the availability of fresh organic matter leads to an increase in benthic biomass. Organic enrichment of sediments surrounding a turbine, and an increase in macrobenthic species richness and biomass have indeed been observed within our studied wind farm^{9,17,18}, but also in a number^{37,42} of windfarms elsewhere (but not all^{43,44}). Our OWF site had the lowest biomass of the studied habitats, predominantly due to the low *E. cordatum* biomass, but given the lack of a true control site (e.g., before-after data) we could not objectively assess changes to the soft-sediment macrofaunal biomass in the studied OWF.

As anticipated, the OWF food web contained more species than the Coarse sandy food web (120 vs. 57 species, Table S. 1–Table S. 3), however, we did not expect such a large difference with the species-rich fine sandy sediment habitat (92 species). Offshore wind foundations, and other hard substrates (e.g., oil and gas platforms) have long been known to, at least locally, increase species richness in a so-called ‘artificial reef effect’^{9,15,45}, and these species all take part in ecological interactions that form the food web. However, compared to the Coarse and Fine sandy food webs, the OWF food web contains more low to very low biomass components, which is due to the presence of rare species on the hard substrates, combined with the species-poor surrounding soft sediments. As the carbon flows to and from these rare groups were also small, values for the average link weights were roughly half those in the Coarse and Fine food web (T_{ij} , Table 1). Interestingly, despite the increased species richness and biomass introduced by the artificial hard substrates and the resulting artificial reef effect, the size of the OWF system is similar to, or equally productive as the Coarse sand system (as expressed by Total System Throughflow TST, Table 1), indicating that these many small flows do contribute to a relevant amount of carbon cycling. Nevertheless, the total carbon throughput in the Fine sandy food web is still 20% higher than in the other two food webs, as a logical consequence of the much higher biomass present in this food web.

Despite the total size of the system, there is evidence that the OWF food web is less stable, or perhaps still less mature in comparison to the other two

food webs. First, the OWF network displays the lowest connectance (CI), a measure of food web complexity, with food web complexity generally regarded as concomitant to stability. The lower connectance may indicate an absence of predatory relations, so that rare species may successfully establish themselves on the hard substrate, which would not be possible on other locations⁴⁶. Possibly, predators may focus on specific, highly preferred prey present in the OWF in high abundance (e.g. *Jassa herdmani*, *Mytilus edulis*), decreasing the number of realized links. With respect to recycling, the revised Finn's cycling index⁴⁷ shows the lowest value for the OWF food web (Table 1), reflecting that in this food web the least amount of carbon is recycled via internal loops. Loops (and especially longer loops consisting of multiple weak interactions) are seen as contributing to network stability, as they ensure that predation pressures are not focused on one individual species, but rather divided⁴⁸. Increased cycling also equates to increased resource storage in a system, and thus the capacity of a system to retain matter and endure whenever oscillating resources become scarce⁴⁹.

Combined, the connectance and recycling properties are expected to become more prominent with increasing food web maturity^{49–51}. Recent research in a wind farm of similar age and in the same area indeed shows that the species community is still evolving, without a clear directionality in the evolution of the macrofaunal species biomass⁵². However, it is theorized that the community eventually reaches a “climax” community dominated by *Mytilus edulis* and *Metridium senile*¹⁶.

We had hypothesized that increased species richness in the OWF food web should lead to increased C throughput and a more complex food web. The OWF food web does indeed display a larger species richness when compared to the surrounding habitats, and the carbon throughput is similar to the coarse sandy habitat where more biomass is present, due to the summation of smaller, though more plentiful flows. However, the network properties indicate that the studied OWF is less stable and/or less mature than the Coarse and Fine sandy food web. Whether these results are a permanent feature of the OWF food web, or a consequence of an evolving species community remains to be seen. In view of anticipated changes in species communities, it could prove useful to look at the evolving OWF food web, so as to discriminate between temporal effects, and effects on the food web that persist throughout the lifetime of the OWF. This requires a substantial monitoring dataset, and an open-source data-policy across institutions and national borders^{44,53}.

Potential benefits for fish

We found a similar biomass in demersal fish in the OWF food web, as in the coarse food web, despite the lower biomass of macrofauna —prey— in the former (in biomass m^{-2} of food web). However, a large part of the biomass discrepancy is due to the much smaller individuals of *E. cordatum* present in the OWF food web. This species, though present in high biomass is apparently not preferred by fish as it was only consumed by Pleuronectidae in the Coarse food web. It is possible that the fish biomass used in this study is an underestimation of the true fish biomass within the OWF, as the values were derived from trawling tracks in between turbines (at 250 m from turbines), whereas the largest fish aggregations are seen directly near the turbines^{11,54}. Standardized fish density assessments this close to the turbine were not available, and therefore they could not be included in the food web model. The OWF food web did contain the highest diversity in fish species, containing some species known to associate with hard-substrates (e.g., *Raniceps raninus*) in addition to the more naturally occurring soft sediment species such as flatfish. Using LIM, we included all observed species in feeding interactions, as LIM does not include non-trophic interactions. In that sense, the model considers the fish community purely from the production side. In the so-called “production-attraction dichotomy”: mobile species such as fish may reside in an area without feeding there, and vice-versa: it may be possible that species feed in an area but predominantly reside elsewhere. For the OWF specifically, there are non-trophic reasons for fish aggregating near turbines, such as shoaling behaviour, availability of shelter, or mate selection. As such the presence of fish can be caused by aggregation, not necessarily leading to increased local productivity^{54,55}.

Refuge effects in offshore wind farms where fishing of any kind is absent, are often most pronounced in fish biomass^{56,57}, without necessarily indicating increased productivity. With this caveat, our model does show a similar production of fish biomass in the OWF food web when compared to the Coarse food web (Table S. 8), meaning that the prey density and diversity within an OWF can potentially sustain all fish biomass present in the area.

A second model observation is that the combined fish species in the OWF food web gather some 25% of their prey from the hard substrate community, and the majority of prey items are crustaceans (Fig. 5). For several fish groups, the proportion of crustaceans in their diet was higher in the OWF food web, than in the Coarse (e.g. Carangiformes, Gadiformes), and certainly the Fine food web (e.g., Callionymiformes, Carangiformes, Gadiformes, Table S. 12). Recent works in the vicinity of OWFs have shown that certain fish species do indeed adapt their diet to the presence of hard-substrate – associated prey^{10,11}. For example we used the findings of Mavraki et al. (2021)¹⁰ in the feeding matrix to supplement the known prey preference of several fish species in the vicinity of an OWF, such as inclusion of *P. longicornis* in the diet of *M. scorpioides*, and the abundant amphipod *J. herdmani* in the diets of several species. Very high-resolution observations of *Pleuronectes platessa* diurnal migrations also show that these flatfish reside a considerable time on the soft sediments in between wind turbines, with daily migrations to the SPL to feed on specific hard substrate prey types, which is reflected in the stomach contents and fatty acid signature of individuals feeding in these different areas⁵⁸. In our model, the uptake of Pleuronectids (a blend of several flatfish with similar diets in this case), also shows that these species include a variety of hard-substrate species in their diet, though our output does not reflect the high specificity to *Ophiotrix fragilis* apparently displayed by *P. platessa* residing near the turbine¹¹. For this, our LIM model would need to include subsets of Pleuronectids feeding on different locations near the hard substrate, increasing the number of components in a model already approaching the limits of solvability.

Generalizing effects of OWFs on the marine food web

We studied an offshore windfarm located in a shallow (~25 m), nearshore, eutrophic and dynamic environment, a typical setting for fixed offshore-wind turbines⁵⁹. We therefore expect the additional link between water column and the seafloor generated by the epifauna on the turbine foundation and SPL to be a consistent feature of many OWF food webs. Near-shore waters generally tend to be more productive than more offshore areas as well⁶⁰, increasing the food supply to the hard substrate community, and increasing their chances of development, and establishing a similar importance for the soft-substrate community as was observed in our study.

A difference with more recently constructed, and future offshore wind farms is that the densities and species biomass in our study are based on turbine dimensions which are already smaller than recently installed turbines. Towards the future, there is a trend towards even larger turbines for increased energy yield, that have to be spaced further apart to negate efficiency loss^{61,62}. With our current results, it is difficult to make an estimate of the specific scale-dependent effects of turbine dimensions on alterations to the food web. One could expect larger turbines, spaced further apart to have a similar effect on the surrounding food web (per m^{-2}), but the ecological response to these variations in stressor structure will not necessarily be linear⁶³.

In this study we approximated changes to a food web across an OWF, assuming that observations performed on a single turbine are representative for other turbines within that same wind farm. As larger scale studies have shown^{7,8,36,64}, OWF effects on their surroundings tend to dilute with increasing distance away from the OWF. For our OWF, this will likely be at the scale of several kilometres, over which the seafloor C-enrichment effect was modelled to disappear⁶⁴. Whereas effects on the macrofaunal community are unlikely to persist that far, effects on more mobile larger fauna (fish, marine mammals, seabirds) may play out at much larger scales, as a high concentration of prey items may be worth a trip of several 10's of kilometres if it includes their natural foraging area, or is energetically beneficial. Marine mammals and seabirds could not be integrated in our food

web study, as no standardized stock assessments were available. However, it has been described that seals and various seabird species can benefit from the presence of OWFs, whereas other seabird species are negatively affected or react indifferently^{65–67}, with similarly contrasting findings for harbour porpoises (the most common cetacean in the study area)^{68–72}.

Despite our inclusion of a reference site (Coarse) which shared similar grain size characteristics and hydrodynamic setting to the OWF site, this was not a true control site. The different sized *E. cordatum*, much smaller in the OWF sites, caused the OWF to have a lower benthic biomass, which was unexpected. Despite the fact that OWFs are now widespread, and are being constructed on large scale since the late 2000's, true control – impact datasets are needed. Combined with recurrent sampling of the soft- and hard-substrate species (diversity and biomass) throughout the lifetime of an OWF (e.g., every 4 years), such datasets would allow species communities and their functioning to be tracked over time. The temporal dimension would firstly increase the strength of extrapolations towards the future, and secondly result in “current state” assessments that could support policy decisions (e.g. changes to the local dynamics of fish and crustacean populations with economic implications).

Conclusion

Our study reveals the OWF food web as a species rich food web, where a highly concentrated stock of hard-substrate suspension feeding biomass plays a significant role in carbon cycling, despite the limited physical space they occupy in the available habitat. Suspension feeding fauna on the turbine foundation and SPL collect phyto- and zooplankton from the water column, are preyed upon by mobile macrofauna and several fish species, and enrich the surrounding sediment with organic carbon by 8.7–11.6% to the direct benefit of detritivores in the sediment. Despite its high species richness, the OWF food web is less stable than adjacent soft sediment habitats, as indicated by several network indices. This may be a sign that the food web is still evolving towards a stable equilibrium compared to other dynamic marine habitats, or that the large amount of species present in low biomass prevent the formation of more stable links. To constrain changes to trophic interactions in the vicinity of OWFs with certainty, biomass data on the various compartments that make up the OWF food web is needed. This data is sparse, and often depend on research grants for hypothesis driven research (as was the case in the current work). We recommend a fixed monitoring strategy associated with the lifetime of an OWF, where changes to species assemblages can be tracked over time, to have data available that can support ecological research.

Materials and methods

Study sites

The benthic-pelagic food web, from macrofauna to pelagic fish, was sampled in three locations within the Belgian sector of the Southern Bight of the North Sea (SBNS), during August and September of 2016–2017 (Fig. 1). The Coarse location is a coarse sandy sediment site, with a median grain size of $392 \pm 31 \mu\text{m}$ and permeability of $28.5 \pm 2 \cdot 10^{-12} \text{ m}^{-2}$ ³⁰ (historically named “station 330”), and offers habitat to the *Hesionura elongata* community⁷³. The Fine location is defined as a fine-sandy sediment habitat (median grain size: $173 \pm 2 \mu\text{m}$, permeability $0.3 \pm 0.3 \cdot 10^{-12} \text{ m}^{-2}$, “Station 780”³⁰) that is more biomass and species-rich as opposed to the Coarse site, and home to the *Abra alba* community⁷⁴. The OWF site is focused around the “C-Power” windfarm (51 32.88 N 2 55.77 E), which has been the subject of earlier OWF-related studies^{9,15,75}, increasing the amount of available information. The turbines in this wind farm are a mix of gravity based foundations ($n = 6$) and jacket foundations ($n = 48$), however, for the purpose of generality, we chose to model the food web after monopile foundation dimensions, as this is by far the most widely occurring type of foundation, including in the other offshore wind farms in the SBNS. A recent analysis of available data in the study area showed a high similarity between the biofouling community on both foundation types, with differences between surrounding water masses overshadowing the effects of different foundation types⁵². The OWF site contains both the fauna attached to the hard substrate (turbine foundation

+ scour protection layer (SPL)), as well as the surrounding soft sediment (median grain size: $439 \pm 144 \mu\text{m}$, and permeability of $36.3 \pm 20.9 \cdot 10^{-2} \text{ m}^{-2}$ ³⁰) (Fig. 1). We chose this delineation of the OWF food web, as the turbines in this OWF are spaced regularly, 500 meters apart. An OWF may thus be subdivided into units containing a single turbine and the surrounding sediment up to half of the distance towards another turbine. Beyond this distance, the next unit under dominant influence of another turbine begins. The fauna on the hard substrate occurs in a typical depth zonation pattern where species such as *Mytilus edulis*, *Jassa herdmani*, and *Metridium senile* occur roughly in bands, and dominate the biomass^{15,75}. The species community in the surrounding soft sediment also belongs to the *H. elongata* community according to habitat suitability models⁷³, though a shift in species biomass and community appears to be taking place closest to the turbine, towards a community associated with the enrichment effect of the turbines¹⁷.

All chosen locations are well studied in the SBNS, and have recently been thoroughly described in terms of biomass composition and biogeochemical properties^{30,75}.

Food web modelling

Topological food web construction. All species encountered in the different samples were included in the study as food web components. Possible trophic links between different food web components were derived from literature research, by screening the literature for the species name (scientific name and common name, if available), family name, or higher taxon level (if no result from lower levels was found) in combination with the words “diet”, “prey”, “feeding”, and “food”. Ideally, references were found with recordings of stomach contents and observational or experimental determinations of prey preferences of the individual species. If this was not the case, we used studies determining prey preference based on morphology of the feeding apparatus, or assumed a similar feeding preference to closely related species for which information could be found. We also prioritized studies geographically closer to the study site over studies further away (See supplementary references). In the resulting predator-prey interaction matrix, we occasionally noticed an almost complete overlap between the diets of (often related) species. To limit the number of links in the model and avoid excessively long computation times of the LIMs, taxonomically related species with similar feeding preferences were therefore grouped into functional groups to represent a single link in the food web (see Table S. 14, Table S. 15, Table S. 16).

Whereas the Coarse and Fine food webs allowed all macrofauna to interact with each-other as they share the same sediment matrix, macrofauna species on the turbine foundation are separated in space from those in the sediment. Hence species in this food web were separated into interaction groups of “Turbine only”, “Turbine and SPL”, “SPL and soft-sediment”, “soft sediment”, and “ubiquitous” (occurring everywhere).

To close the food webs, additional components were introduced for water column bacteria, sediment bacteria, sedOM (sediment organic matter), watPOM (suspended POM in the water column), and DIC (Dissolved Inorganic Carbon resulting from respiration) in the water column. sedOM and watPOM are detrital food sources for fauna in the sediment and water column respectively. In turn, dead organisms and (pseudo-)faeces contribute to the detrital pools where they occur. The detrital pools form the food source for bacteria in the water column or in the sediment. Bacteria remineralize sedOM and watPOM to DIC (available for uptake by phytoplankton), however the incomplete mineralization of OM in the sediment leads to a certain amount of burial in sediments (Figure S. 2).

With the collected sampling data, supplemented with literature information, a linear inverse model (LIM²⁶) was constructed to estimate carbon flows between individual food web components.

Linear inverse modelling. Linear inverse models (LIM) were constructed from the topological food webs developed in the previous section, following Soetaert & van Oevelen (2009) and De Smet et al. (2016).

In LIMs, unknown flows between food web components are constrained by observational data collected from the system, which in this case were measurements of the stocks of the food web components, measured isotopic compositions, and known bounds to physiological processes.

Mathematically, the carbon flows (in $\text{mmol C m}^{-2} \text{ d}^{-1}$) in the food web are cast in matrix notation as a set of linear equalities (1) and inequalities (2)²⁴:

$$A \cdot x = b \quad (1)$$

$$G \cdot x \geq h \quad (2)$$

where x is a vector with N unknown food web flows. Each row in matrix A is a mass balance or data point expressed as a linear combination of the food web flows, where the corresponding rate of change of a compartment (for mass balances) or numerical value (for data equalities) is given in vector b . h is a vector containing values for biological constraints, and the constraint coefficients, signifying whether and how much a flow contributes to the constraint, are given in matrix G . Equalities contain quantitative site-specific data such as the species biomass and $\delta^{15}\text{N}$ values of the different compartments. Isotopic values can be used to constrain the specific prey consumed by an organism out of a pool of possible prey types^{76–79}. Inequalities contain lower and upper bounds of physiological processes (production rates, assimilation efficiencies, respiration rates) derived from literature, since they are used to constrain single flows or linear combinations of flows to biologically realistic values. The specific inequalities were respiration rates of fauna and the sediment community, and literature-derived process rate constants described below. All variables (respiration, uptake, assimilation, production) are expressed in units of $\text{mmol C m}^{-2} \text{ d}^{-1}$, as a result of the multiplication of rate constants (d^{-1}) with stocks of fauna, bacteria, detrital sources, phytoplankton, or DIC, expressed in mmol C m^{-2} , or multiplication of a dimensionless constant (e.g. assimilation proportion) with a flow (expressed in $\text{mmol C m}^{-2} \text{ d}^{-1}$).

Respiration was added for each functional group to the LIM to calculate the biomass production of the food web components. Biomass production results from the difference between assimilated carbon (total prey uptake minus (pseudo)defecation), and respiration needed to sustain the metabolism of the current biomass.

For macrofauna the respiration rate was calculated using the following formula⁸⁰ (3), valid for shallow water organisms in a 15–20 °C temperature range:

$$r = 0.017 \cdot W^{-0.156} \quad (3)$$

with r the biomass specific respiration rate (d^{-1}) and W the individual biomass (mg C ind^{-1}). The respiration ($\text{mmol C m}^{-2} \text{ d}^{-1}$) results from the multiplication of r with the biomass of the given species. Lower and upper bounds to the respiration rates were set as $R \cdot 0.75$ (minResp) and $R \cdot 1.25$ (maxResp) respectively²⁶.

For larger organisms (fish) a respiration rate of 0.01 (d^{-1}) was taken⁸¹.

Total sediment community oxygen consumption (SCOC) measurements measured at each of the studied locations in 2016/2017³⁰ were used to constrain total respiration rates of the combined macrofauna and sediment bacteria components, i.e. we instructed the LIM to keep the sum of all components consuming oxygen in the sediment as close as possible to oxygen consumption rates of the total community measured in experimental units.

Additionally, a number of general inequality constraints was taken from literature to constrain bacterial growth efficiency, assimilation, and production efficiency of all faunal compartments (Table S. 17)^{78,82}.

A parsimonious solution to the system of equations and inequalities was acquired through least distance programming, i.e., by minimizing the sum of the squared unknowns (the flows, x_i):

$$\min \left(\sum \text{Cost}_i \cdot x_i^2 \right) \quad (4)$$

Since our LIMs were of underdetermined nature (number of equations was less than the number of flows to be estimated, see Table S. 18), multiple solutions were possible, each consistent with the equality and inequality constraints of the matrix. The parsimonious solutions were used to initialize a Monte Carlo Markov Chain (MCMC) method to explore the solution space further⁸³. For each food web, the MCMCs were performed to generate 10000 possible solutions that satisfied the constraints of the LIM, resulting in a distribution of estimates for each individual flow from which a reliable mean and standard deviation of each flow could be calculated^{83,85}.

Convergence of the solutions towards consistent flow means and standard deviations was checked to confirm that our 10,000 solutions were sufficient⁸⁴. For the three food webs, model convergence within 10% of the final mean and standard deviation for each flow value was achieved after 2000 solutions (Figure S. 3), which we considered as successful convergence⁸⁴. After 10,000 solutions the variance of the standard deviation for a given flow solution was 4% or less of the variance on the standard deviations of 50 randomly sampled solutions.

LIMs were solved using the LIM package⁸⁵, using R⁸⁶ and RStudio⁸⁷. To speed up the MCMC, solutions were run on the HPC cluster of the Royal Netherlands Institute of Sea Research (NIOZ).

Availability of data

Stock data. The measurements of species biomass as described above were used as stock data of the different food web components. In case of missing biomasses, these were taken from previous works in the area, or from measurements collected in an OWF in the Dutch part of the North Sea (See Table S. 1, Table S. 2, Table S. 3 for the species biomass, calculated respiration rates, and alternative source if not originally from this work). Species densities and biomass in the OWF domain, were standardized to their respective surface of occurrence (Table S. 19, Figure S1). Weights of macrofauna and epifauna were converted to carbon units using published conversion factors for aquatic organisms⁸⁸.

Data on fish densities and length classes were provided by ILVO (Institute of Agriculture and Fisheries Research), who perform annual trawl surveys in the area of interest. From this information, biomass was derived by using published length-weight relationships for the different species⁸⁹. Fish weights were converted to carbon units (mmol C m^{-2}) using appropriate conversion factors⁹⁰.

An available dataset based on zooplankton field samples collected with a WP2 net showed a very limited number of individuals present. To provide more realistic values to these observations, jellyfish biomass and densities were estimated from gelatinous plankton densities recorded for the SBNS⁹¹. Eventually, due to the mixed nature of the SBNS, we chose to use the same three species for all stations, corresponding to very common species, and average weights for these jellyfish species were then found in various published references^{92–94}. Finally a jellyfish WW to C conversion factor was used⁹⁵ (see supplementary Table S. 20 for the jellyfish recalculations).

Zooplankton stocks were estimated from Schrum et al.⁹⁶. Phytoplankton biomass was converted from water column chlorophyll a concentrations measured in the area by Toussaint et al. (unpubl.), by using a published conversion factor of chlorophyll to phytoplankton⁹⁷. To maximize comparability of results between the different food webs, the initial input of carbon into the food web (primary productivity, i.e. the flow representing net uptake of DIC by phytoplankton), was fixed for the three locations at $250 \text{ mmol C m}^{-2} \text{ d}^{-1}$ ⁹⁸, assuming a well-mixed water column in the SBNS⁹⁹ and no physiological differences between phytoplankton communities over such short distances.

The stocks of sediment organic matter reported in Toussaint et al. (2021) were converted to the model units. For water column organic matter, we used values sampled specifically in the Coarse station by van Oevelen et al. (2009) (see Table S. 21 for the calculations for zooplankton, phytoplankton, sedOM and watPOM).

Finally, bacterial biomass in water and sediment were derived from Billen¹⁰⁰ (see Table S. 22). For water bacteria, the biomass was constant for the three sites, and the average value reported in Table 1 of Billen et al. (1990)

of $\pm 30 \mu\text{gC L}^{-1}$ for the BPNS was converted to mmol C m^{-3} . For sediment bacterial biomass, the relationship between sediment organic matter content (mg cm^{-3}) and bacterial biomass ($\mu\text{gC cm}^{-3}$) reported in Figure 18 of Billen et al. (1990) was used to convert organic matter contents reported in Toussaint et al. (2021) to bacterial biomass in the sediment.

Species collection for stable isotope analysis. To acquire $\delta^{15}\text{N}$ data from each of the food web compartments, dedicated field samplings were carried out in September 2016 and 2017. The water column was sampled for watPOM and zooplankton, and pelagic fish, while the turbine foundation was sampled for colonizing macrofauna and the sediment for sedOM, macrobenthos, demersal fish and epibenthos.

One otter trawl at the Coarse and Fine location, and two within the OWF location (250 m away from the turbines) were performed to collect fish (see Table S. 23 for otter trawl location and track length, Figure S. 4 for locations in OWF). Once on the vessel, organisms were sorted and identified to species level where possible. Trawling was supplemented with long-line fishing to include pelagic fish to the study using *Arenicola marina* as bait, and a variety of artificial bait types. Fish were identified on board. A minimum of five individuals of each species was selected for stable isotope analysis (SIA below). For all fish species, part of the dorsal muscle (without skin) was collected for at least 5 individuals per species.

Zooplankton was collected from vertical hauls across the entire water column with a WP2 plankton net ($\varnothing 0.57 \text{ m}^2$, mesh size of $200 \mu\text{m}$). The net was lowered down to 3 m above the seafloor, and slowly recovered. The zooplankton samples were then concentrated by sieving over different mesh sizes (800 and $250 \mu\text{m}$), and organisms were starved in filtered in situ seawater ($0.45 \mu\text{m}$ GF/F filter) to allow for gut clearance overnight, for subsequent analysis of isotopic composition¹⁰¹. In the lab, the collected benthic organisms, and jellyfish collected in the WP2 net were identified up to lowest taxonomic level using field guides and where needed, under a stereo microscope.

For watPOM, 5 L of bottom water were collected and pre-filtered with a $63 \mu\text{m}$ sieve to remove any zooplankton or algal debris. watPOM was extracted from the water via filtration through precombusted and pre-weighed Whatman GF/C filters.

Fauna in the sediment was collected with a NIOZ boxcorer ($\varnothing 30 \text{ cm}$) and a Van Veen grab (0.1 m^2), in the wind farm this was done at 200 m SW of the turbine. At each study site triplicate samples were collected with each device. The boxcore samples were then sieved over a 1 mm sieve and the collected macrofauna were stored frozen at -20°C until identification. The boxcores were also subsampled for environmental characteristics, including the sediment organic matter (sedOM) content, which was also analyzed for stable isotope ratios. The macrobenthos from the Van Veen samples was extracted by decantation, by collecting them into a large bucket and topping off with water, and swirling around the bucket and picking out fauna from the water. This step was repeated 10 times or until no new organisms surfaced. The remaining content of the buckets was sieved over a 1 mm sieve, and fauna were collected. Fauna was separated into morphospecies on board, and processed further for stable isotope analysis. All smaller organisms were sorted into lowest taxonomical groups possible after sampling, left overnight in filtered sea water ($0.45 \mu\text{m}$ GF/F filter) for gut evacuation and subsequently frozen (-20°C) in vials filled with fresh filtered sea water. Within each taxon only organisms of similar size were used for SIA to avoid possible isotopic signature changes due to ontogenetic shifts¹⁰². Extended details on sampling and lab procedures are described elsewhere^{10,75}. Eventually, the biomass and species densities of each species were derived from all samples.

To sample the community inhabiting the turbine foundation, a combination of scraping the turbine surface of the intertidal zone from aboard a rubber hulled inflatable boat, and sample collection by scientific divers was used to sample the turbine at 5, 8.5, 15–20, and 25–27 m water depth⁷⁵. Larger crustaceans collected by divers were immediately freeze-killed and cheliped tissue was subsequently collected for SIA analysis. Extended details on the sampling of macrofauna and water column suspended matter can be found in

Toussaint et al. (2021)³⁰ for the Coarse, Fine, and sediment surrounding the OWF site, and in Mavraki et al. (2020, 2021)^{10,75} for the turbine itself.

Sample analysis

Staple isotope composition. To determine the $\delta^{15}\text{N}$ signature, individual organisms and muscle tissue samples were defrosted and rinsed with milli-Q to avoid cross-contamination, and dried at 60°C for 12–48 hours depending on their size. Dried samples were powderized with a glass mortar and pestle. 1 mg of powderized sample was then placed in pre-weighed Sn cups, before storage in multi-well Microtitre plates in a desiccator until further analysis^{103,104}.

For the watPOM $\delta^{15}\text{N}$ values, filters were dried for 24 h at 60°C . Half of the filter, reserved for this specific analysis, was then placed in a tin (Sn) capsule and stored.

The samples were analyzed on a PDZ Europa ANCA GSL elemental analyzer, interfaced to a PDZ Europa 20–20 isotope ratio mass spectrometer at the UC Davis Stable Isotope Facility (University of California, USA). Eventually the nitrogen isotope ratio was expressed in the standard delta (δ) notation (5):

$$\delta^{15}\text{N} = \left[\left(\frac{R_{\text{Sample}}}{R_{\text{Standard}}} \right) - 1 \right] \cdot 10^3 \quad (5)$$

where R is the ratio of $^{15}\text{N}/^{14}\text{N}$ of the sample or the reference standard, expressed in %.

nMDS representation of biomass

To visualise the differences between the species communities between the food webs, we used a non-metric multidimensional scaling (nMDS) of the faunal biomass densities. The metaMDS function from the R package 'vegan'¹⁰⁵ was used, with Bray-Curtis dissimilarity.

Calculation of network indices

Several network indices were calculated to evaluate structural and functional differences between the different food webs: Total system throughflow (TST , the sum of all compartmental/nodal carbon inputs), the total number of links (L_{tot}), the number of internal links (L_{int} , does not include fluxes to or from externals), the link density (LD , average number of links per compartment), the average link weight (T_{ij} , a measure of the average flow through a food web component), the connectance (CI , the fraction of all possible links realized in the food web), and the revised Finn's cycling index (FCI , a measure of the retentiveness of a system). The indices were calculated on the averaged output of the Monte Carlo simulations, using the 'NetIndices' package²⁹ available in R. See Kones et al. (2009) for the formulas behind each index.

Intermodel comparison of results. To test the hypotheses, the variables resulting from the three models were compared by calculating the fraction of which the randomized set of 1000 results of one model is larger than that of another model. For example, when this fraction is 0.90, this implies that 90% of the values of model 1 are larger than the ones of model 2 (and consequently, 10% of the values are lower). We define differences of 90% and 10% as significant difference and 95% and 5% as highly significant difference.

To compare the diets of fish species in different food webs, a PERMANOVA test, followed by a pairwise PERMANOVA was performed to test for significant differences in the proportion of major food groups in the species' diet, followed by a SIMPER analysis to highlight the specific diet components contributing most to this difference. Both analyses were performed with 999 permutations of 1000 randomly selected model solutions from each food web. Flows were transformed to proportions of total food intake per species, and Bray-Curtis dissimilarity was used as a distance matrix for both analyses. These analyses were performed in the R package 'vegan'¹⁰⁵.

Data availability

Data tables containing information used to construct the food webs (species biomass and densities, isotopic values, topological food web relations) are available under CC-BY 4.0 license in the following repository: <https://doi.org/10.6084/m9.figshare.c.7722626.v1>¹⁰⁶.

Code availability

Input files and code to reproduce results reported in the article are available under the following Github repository under a CC-BY 4.0 license: <https://doi.org/10.5281/zenodo.15042067>¹⁰⁷.

Received: 18 July 2024; Accepted: 27 March 2025;

Published online: 29 April 2025

References

- Williams, R. & Zhao, F. *Global Offshore Wind Report 2023*. 117 <https://gwec.net/gwecs-global-offshore-wind-report-2023/> (2023).
- Putuhen, H., White, D., Gourvenec, S. & Sturt, F. Finding space for offshore wind to support net zero: A methodology to assess spatial constraints and future scenarios, illustrated by a UK case study. *Renew. Sustain. Energy Rev.* **182**, 113358 (2023).
- Degraer, S. et al. Offshore Wind Farm Artificial Reefs Affect Ecosystem Structure and Functioning: A Synthesis. *Oceanography* **33**, 48–57 (2020).
- Voet, H., Van Colen, C. & Vanaverbeke, J. Climate change effects on the ecophysiology and ecological functioning of an offshore wind farm artificial hard substrate community. *Sci. Total Environ.* **810**, 152194 (2021).
- Mavraki, N. et al. Small suspension-feeding amphipods play a pivotal role in carbon dynamics around offshore man-made structures. *Mar. Environ. Res.* **178**, 105664 (2022).
- Clausen, I. & Riisgård, H. Growth, filtration and respiration in the mussel *Mytilus edulis*: no evidence for physiological regulation of the filter-pump to nutritional needs. *Mar. Ecol. Prog. Ser.* **141**, 37–45 (1996).
- Slavik, K. et al. The large scale impact of offshore windfarm structures on pelagic primary production in the southern North Sea. *Hydrobiologia* **845**, 35–53 (2019).
- van Duren, L. A. et al. *Ecosystem Effects of Large Upscaling of Offshore Wind on the North Sea - Synthesis Reports*. **42**, <https://www.noordzeeloket.nl/publish/pages/190265/synthesis-ecosystem-effects-of-large-upscaling-of-offshore-wind-on-the-north-sea.pdf> (2021).
- Coates, D. A., Deschutter, Y., Vincx, M. & Vanaverbeke, J. Enrichment and shifts in macrobenthic assemblages in an offshore wind farm area in the Belgian part of the North Sea. *Mar. Environ. Res.* **95**, 1–12 (2014).
- Mavraki, N., Degraer, S. & Vanaverbeke, J. Offshore wind farms and the attraction–production hypothesis: insights from a combination of stomach content and stable isotope analyses. *Hydrobiologia* **848**, 1639–1657 (2021).
- Buyse, J., Hostens, K., Degraer, S., De Troch, M. & De Backer, A. Increased food availability at offshore wind farms affects trophic ecology of plaice *Pleuronectes platessa*. *Sci. Tot. Environ.* 160730 <https://doi.org/10.1016/j.scitotenv.2022.160730> (2022).
- Gimpel, A. et al. Ecological effects of offshore wind farms on Atlantic cod (*Gadus morhua*) in the southern North Sea. *Sci. Total Environ.* **878**, 162902 (2023).
- Reubens, J. T., Degraer, S. & Vincx, M. Aggregation and feeding behaviour of pouting (*Trisopterus luscus*) at wind turbines in the Belgian part of the North Sea. *Fish. Res.* **108**, 223–227 (2011).
- Reubens, J. T. et al. Aggregation at windmill artificial reefs: CPUE of Atlantic cod (*Gadus morhua*) and pouting (*Trisopterus luscus*) at different habitats in the Belgian part of the North Sea. *Fish. Res.* **139**, 28–34 (2013).
- De Mesel, I., Kerckhof, F., Norro, A., Rumes, B. & Degraer, S. Succession and seasonal dynamics of the epifauna community on offshore wind farm foundations and their role as stepping stones for non-indigenous species. *Hydrobiologia* **756**, 37–50 (2015).
- Kerckhof, F., Rumes, B. & Degraer, S. About ‘Mytilisation’ and ‘slimeification’: a decade of succession of the fouling assemblages on wind turbines off the Belgian coast. in *Environmental Impacts of Offshore Wind Farms in the Belgian Part of the North Sea: Marking a Decade of Monitoring, Research and Innovation* (eds. Degraer, S., Brabant, R., Rumes, B. & Vigin, L.) 134 (Royal Belgian Institute of Natural Sciences, OD Natural environment, Brussels, 2019).
- Lefaille, N., Braeckman, U., Degraer, S., Vanaverbeke, J. & Moens, T. A wind of change for soft-sediment infauna within operational offshore windfarms. *Mar. Environ. Res.* **188**, 106009 (2023).
- Braeckman, U., Lefaille, N., Bruns, E. & Moens, T. Turbine-related impacts on macrobenthic communities: an analysis of spatial and temporal variability. in *Environmental Impacts of Offshore Wind Farms in the Belgian Part of the North Sea: Empirical Evidence Inspiring Priority Monitoring, Research and Management*. (eds. Degraer, S., Brabant, R., Rumes, B. & Vigin, L.) (Royal Belgian Institute of Natural Sciences, OD NATural environment, Brussels, 2020).
- Mavraki, N., Degraer, S., Moens, T. & Vanaverbeke, J. Functional differences in trophic structure of offshore wind farm communities: A stable isotope study. *Mar. Environ. Res.* **157**, 104868 (2020).
- Raoux, A. et al. Benthic and fish aggregation inside an offshore wind farm: Which effects on the trophic web functioning?. *Ecol. Indic.* **72**, 33–46 (2017).
- Halouani, G. et al. A spatial food web model to investigate potential spillover effects of a fishery closure in an offshore wind farm. *J. Mar. Syst.* **212**, 103434 (2020).
- Wang, L. et al. Ecological impacts of the expansion of offshore wind farms on trophic level species of marine food chain. *J. Environ. Sci.* **139**, 226–244 (2024).
- Pezy, J. -P., Raoux, A. & Dauvin, J. -C. An ecosystem approach for studying the impact of offshore wind farms: a French case study. *ICES J. Mar. Sci.* **77**, 1238–1246 (2020).
- Vézina, A. F. & Platt, T. Food web dynamics in the ocean. I. Best-estimates of flow networks using inverse methods. *Mar. Ecol. Prog. Ser.* **42**, 269–287 (1988).
- van Oevelen, D. et al. Quantifying Food Web Flows Using Linear Inverse Models. *Ecosystems* **13**, 32–45 (2010).
- Soetaert, K. & van Oevelen, D. Modeling Food Web Interactions in Benthic Deep-Sea Ecosystems: A Practical Guide. *Oceanog* **22**, 128–143 (2009).
- Finn, J. T. Measures of ecosystem structure and function derived from analysis of flows. *J. Theor. Biol.* **56**, 363–380 (1976).
- Patten, B. C. *Systems Analysis and Simulation in Ecology: Volume IV*. (Elsevier, 2013).
- Kones, J. K., Soetaert, K., van Oevelen, D. & Owino, J. O. Are network indices robust indicators of food web functioning? A Monte Carlo approach. *Ecol. Model.* **220**, 370–382 (2009).
- Toussaint, E. et al. Faunal and environmental drivers of carbon and nitrogen cycling along a permeability gradient in shallow North Sea sediments. *Sci. Total Environ.* **767**, 144994 (2021).
- Krone, R., Gutow, L., Joschko, T. J. & Schröder, A. Epifauna dynamics at an offshore foundation – Implications of future wind power farming in the North Sea. *Mar. Environ. Res.* **85**, 1–12 (2013).
- Rumes, B. et al. Does it really matter? Changes in species richness and biomass at different spatial scales. In *Environmental impacts of offshore wind farms in the Belgian part of the North Sea: Learning from the past to optimise future monitoring programmes* (eds Degraer, S., Brabant, R. & Rumes B.) 182–189 (Royal Belgian Institute of Natural Sciences, 2013).

33. De Backer, A. et al. *Ecological Assessment of Intense Aggregate Dredging Activity on the Belgian Part of the North Sea*. https://pure.ilvo.be/ws/portafiles/porta/5715271/Report_studyday_2017_with_contributions_ILVO.pdf (2017).
34. Newell, R., Seiderer, L. & Hitchcock, D. The impact of dredging works in coastal waters: a review of the sensitivity to disturbance and subsequent recovery of biological resources on the sea bed. *Oceanogr. Mar. Biol.* **36**, 127–178 (1998).
35. Foden, J., Rogers, S. I. & Jones, A. P. Recovery rates of UK seabed habitats after cessation of aggregate extraction. *Mar. Ecol. Prog. Ser.* **390**, 15–26 (2009).
36. Ivanov, E. et al. Offshore Wind Farm Footprint on Organic and Mineral Particle Flux to the Bottom. *Front. Marine Sci.* <https://doi.org/10.3389/fmars.2021.631799> (2021).
37. Maar, M., Bolding, K., Petersen, J. K., Hansen, J. L. S. & Timmermann, K. Local effects of blue mussels around turbine foundations in an ecosystem model of Nysted off-shore wind farm, Denmark. *J. Sea Res.* **62**, 159–174 (2009).
38. Boudreau, B. P. et al. Permeable marine sediments: Overturning an old paradigm. *Eos, Trans. Am. Geophys. Union* **82**, 133–136 (2001).
39. Huettel, M., Berg, P. & Kostka, J. E. Benthic Exchange and Biogeochemical Cycling in Permeable Sediments. *Annu. Rev. Mar. Sci.* **6**, 23–51 (2014).
40. Provoost, P. et al. Modelling benthic oxygen consumption and benthic-pelagic coupling at a shallow station in the southern North Sea. *Estuar., Coast. Shelf Sci.* **120**, 1–11 (2013).
41. Braeckman, U. et al. Variable Importance of Macrofaunal Functional Biodiversity for Biogeochemical Cycling in Temperate Coastal Sediments. *Ecosystems* **17**, 720–737 (2014).
42. Hutchison, Z. et al. Offshore Wind Energy and Benthic Habitat Changes: Lessons from Block Island Wind Farm. *Oceanography* **33**, 58–69 (2020).
43. IMARES Onderzoeksformatie, Jak, R. & Glorius, S. *Macrobenthos in Offshore Wind Farms: A Review of Research, Results and Relevance for Future Developments*. <https://research.wur.nl/en/publications/30bdca91-6754-49ff-9b98-d85eb4b1a0ec> 10.18174/415357 (2017).
44. Coolen, J. W. P. et al. Generalized changes of benthic communities after construction of wind farms in the southern North Sea. *J. Environ. Manag.* **315**, 115173 (2022).
45. De Backer, A., Buyse, J. & Hostens, K. A decade of soft sediment epibenthos and fish monitoring at the Belgian offshore wind area. in *Environmental Impacts of Offshore Wind Farms in the Belgian Part of the North Sea: Empirical Evidence Inspiring Priority Monitoring, Research and Management*. (eds. Degraer, S., Brabant, R., Rumes, B. & Vigin, L.) (Royal Belgian Institute of Natural Sciences, OD Natural environment, Brussels, 2020).
46. Dunne, J. A., Williams, R. J. & Martinez, N. D. Food-web structure and network theory: The role of connectance and size. *Proc. Natl. Acad. Sci.* **99**, 12917–12922 (2002).
47. Allesina, S. & Ulanowicz, R. E. Cycling in ecological networks: Finn's index revisited. *Computational Biol. Chem.* **28**, 227–233 (2004).
48. Neutel, A. -M., Heesterbeek, J. A. P. & de Ruiter, P. C. Stability in Real Food Webs: Weak Links in Long Loops. *Science* **296**, 1120–1123 (2002).
49. Odum, E. P. The Strategy of Ecosystem Development: An understanding of ecological succession provides a basis for resolving man's conflict with nature. *Science* **164**, 262–270 (1969).
50. Finn, J. T. Flow Analysis of Models of the Hubbard Brook Ecosystem. *Ecology* **61**, 562–571 (1980).
51. Christensen, V. Ecosystem maturity — towards quantification. *Ecol. Model.* **77**, 3–32 (1995).
52. Zupan, M., Rumes, B., Vanaverbeke, J., Degraer, S. & Kerckhof, F. Long-Term Succession on Offshore Wind Farms and the Role of Species Interactions. *Diversity* **15**, 288 (2023).
53. Dannheim, J. et al. Biodiversity Information of benthic Species at Artificial structures – BISAR. *Sci. Data* **12**, 604 (2025).
54. Reubens, J. T., Degraer, S. & Vincx, M. The ecology of benthopelagic fishes at offshore wind farms: a synthesis of 4 years of research. *Hydrobiologia* **727**, 121–136 (2014).
55. Schwartzbach, A., Behrens, J. & Svendsen, J. Atlantic cod *Gadus morhua* save energy on stone reefs: implications for the attraction versus production debate in relation to reefs. *Mar. Ecol. Prog. Ser.* **635**, 81–87 (2020).
56. Florin, A. -B., Bergström, U., Ustups, D., Lundström, K. & Jonsson, P. R. Effects of a large northern European no-take zone on flatfish populations. *a. J. Fish. Biol.* **83**, 939–962 (2013).
57. Murawski, S. A. & Fogarty, M. J. Do Marine Protected Areas Really Work? <https://www.whoi.edu/oceanus/feature/do-marine-protected-areas-really-work/> (2005).
58. Buyse, J. et al. European plaice movements show evidence of high residency, site fidelity, and feeding around hard substrates within an offshore wind farm. *ICES J. Marine Sci.* 1–13 <https://doi.org/10.1093/icesjms/fsad179> (2023).
59. Moore, A., Price, J. & Zeyringer, M. The role of floating offshore wind in a renewable focused electricity system for Great Britain in 2050. *Energy Strategy Rev.* **22**, 270–278 (2018).
60. Sigman, D. M. & Hain, M. P. The Biological Productivity of the Ocean. *Nat. Educ. Knowl.* **3**, 21 (2012).
61. Akhtar, N., Geyer, B. & Schrum, C. Larger wind turbines as a solution to reduce environmental impacts. *Sci. Rep.* **14**, 6608 (2024).
62. Gielen, D. et al. *Future of Wind: Deployment, Investment, Technology, Grid Integration and Socio-Economic Aspects*. **87** https://www.irena.org/-/media/Files/IRENA/Agency/Publication/2019/Oct/IRENA_Future_of_wind_2019.pdf (2019).
63. Hunsicker, M. E. et al. Characterizing driver–response relationships in marine pelagic ecosystems for improved ocean management. *Ecol. Appl.* **26**, 651–663 (2016).
64. De Borger, E. et al. Offshore Windfarm Footprint of Sediment Organic Matter Mineralization Processes. *Front. Marine Sci.* **8**, 2539–2557 (2021).
65. Vanermen, N., Courtens, W., Van De Walle, M., Verstraete, H. & Stienen, E. Seabird monitoring at the Thornton Bank offshore wind farm: Updated seabird displacement results as an explorative assessment of large gull behaviour inside the wind farm area. in *Environmental impacts of offshore wind farms in the Belgian Part of the North Sea: A continued move towards integration and quantification* (eds. Degraer, S., Brabant, R., Rumes, B. & Vigin, L.) 85–114 (Royal Belgian Institute of Natural Sciences, OD Natural environment, Brussels, 2017).
66. Vanermen, N., Courtens, W., Van De Walle, M., Verstraete, H. & Stienen, E. Seabirds and offshore wind farms - the potential value of sensitivity mapping in marine spatial planning. in *Environmental impacts of offshore wind farms in the Belgian Part of the North Sea: Getting ready for offshore wind farm expansion in the North Sea* 55–67 (Royal Belgian Institute of Natural Sciences, OD Natural environment, Brussels, 2022).
67. Russell, D. J. F. et al. Marine mammals trace anthropogenic structures at sea. *Curr. Biol.* **24**, R638–R639 (2014).
68. Haelters, J., Paoletti, S., Laurence, V. & Rumes, B. Seasonal distribution of harbour porpoises (*Phocoena phocoena*) and response to operational offshore wind farms in the Belgian North Sea. in *Environmental Impacts of Offshore Wind Farms in the Belgian Part of the North Sea: Progressive insights in changing species distribution patterns informing marine management* (eds. Degraer, S., Brabant, R., Rumes, B. & Vigin, L.) 61–83 (Royal Belgian Institute of Natural Sciences, OD Natural environment, Brussels, 2023).
69. van Polanen Petel, T., Geelhoed, S. & Meesters, E. *Harbour Porpoise Occurrence in Relation to the Prinses Amaliawindpark*. **34**, 1–34 (2012).

70. Teilmann, J. & Carstensen, J. Negative long term effects on harbour porpoises from a large scale offshore wind farm in the Baltic—evidence of slow recovery. *Environ. Res. Lett.* **7**, 045101 (2012).
71. Vallejo, G. C. et al. Responses of two marine top predators to an offshore wind farm. *Ecol. Evolution* **7**, 8698–8708 (2017).
72. Dähne, M. et al. Marine mammals and windfarms: Effects of alpha ventus on harbour porpoises. in *Ecological Research at the Offshore Windfarm alpha ventus* (eds. Federal Maritime And Hydrographic A & Federal Ministry For The Environment) 133–149 (Springer Fachmedien Wiesbaden, Wiesbaden, 2014). https://doi.org/10.1007/978-3-658-02462-8_13.
73. Breine, N. T. et al. Structural and functional diversity of soft-bottom macrobenthic communities in the Southern North Sea. *Estuar., Coast. Shelf Sci.* **214**, 173–184 (2018).
74. Van Hoey, G., Degraer, S. & Vincx, M. Macrobenthic community structure of soft-bottom sediments at the Belgian Continental Shelf. *Estuar., Coast. Shelf Sci.* **59**, 599–613 (2004).
75. Mavraki, N., De Mesel, I., Degraer, S., Moens, T. & Vanaverbeke, J. Resource Niches of Co-occurring Invertebrate Species at an Offshore Wind Turbine Indicate a Substantial Degree of Trophic Plasticity. *Front. Mar. Sci.* **7**, 379 (2020).
76. Braeckman, U. et al. Glacial melt impacts carbon flows in an Antarctic benthic food web. *Front. Mar. Sci.* **11**, 1–19 (2024).
77. Eldridge, P., Cifuentes, L. & Kaldy, J. Development of a stable-isotope constraint system for estuarine food-web models. *Mar. Ecol. Prog. Ser.* **303**, 73–90 (2005).
78. Oevelen, D. et al. Carbon flows through a benthic food web: Integrating biomass, isotope and tracer data. *J. Mar. Res.* **64**, 453–482 (2006).
79. van Oevelen, D. et al. Organic matter input and processing in two contrasting North Sea sediments: insights from stable isotope and biomass data. *Mar. Ecol. Prog. Ser.* **380**, 19–32 (2009).
80. Mahaut, M. -L., Sibuet, M. & Shirayama, Y. Weight-dependent respiration rates in deep-sea organisms. *Deep Sea Res. Part I: Oceanographic Res. Pap.* **42**, 1575–1582 (1995).
81. De Smet, B., van Oevelen, D., Vincx, M., Vanaverbeke, J. & Soetaert, K. Lanice conchilega structures carbon flows in soft-bottom intertidal areas. *Mar. Ecol. Prog. Ser.* **552**, 47–60 (2016).
82. Oevelen, D. et al. The cold-water coral community as hotspot of carbon cycling on continental margins: A food-web analysis from Rockall Bank (northeast Atlantic). *Limnol. Oceanogr.* **54**, 1829–1844 (2009).
83. Kones, J. K., Soetaert, K., van Oevelen, D., Owino, J. O. & Mavuti, K. Gaining insight into food webs reconstructed by the inverse method. *J. Mar. Syst.* **60**, 153–166 (2006).
84. van Oevelen, D. et al. Carbon flows in the benthic food web at the deep-sea observatory HAUSGARTEN (Fram Strait). *Deep Sea Res. Part I: Oceanogr. Res. Pap.* **58**, 1069–1083 (2011).
85. Oevelen, D. et al. Quantifying Food Web Flows Using Linear Inverse Models. *Ecosystems* **13**, 32–45 (2010).
86. R Core Team. *R: A Language and Environment for Statistical Computing*. (R Foundation for Statistical Computing, Vienna, Austria, 2021).
87. Posit team. *RStudio: Integrated Development Environment for R*. (Posit Software, PBC, Boston, MA, 2022).
88. Brey, T., Müller-Wiegmann, C., Zittier, Z. M. C. & Hagen, W. Body composition in aquatic organisms — A global data bank of relationships between mass, elemental composition and energy content. *J. Sea Res.* **64**, 334–340 (2010).
89. Froese, R. & Pauly, D. Fishbase. *FishBase* <https://www.fishbase.org> (2022).
90. Ikeda, T., McKinnon, A. D. & Doherty, P. J. Metabolism and chemical composition of small teleost fishes from tropical inshore waters. *Mar. Ecol. Prog. Ser.* **435**, 197–207 (2011).
91. Vansteenberghe, L., Van Regenmortel, T., De Troch, M., Vincx, M. & Hostens, K. Gelatinous zooplankton in the Belgian part of the North Sea and the adjacent Schelde estuary: Spatio-temporal distribution patterns and population dynamics. *J. Sea Res.* **97**, 28–39 (2015).
92. Buecher, E., Sparks, C., Brierley, A., Boyer, H. & Gibbons, M. Biometry and size distribution of Chrysaora hysoscella (Cnidaria, Scyphozoa) and Aequorea aequorea (Cnidaria, Hydrozoa) off Namibia with some notes on their parasite Hyperia medusarum. *J. Plankton Res.* **23**, 1073–1080 (2001).
93. Mutlu, E. & Bingel, F. Distribution and abundance of ctenophores, and their zooplankton food in the Black Sea. I. Pleurobrachia pileus. *Mar. Biol.* **135**, 589–601 (1999).
94. Shiganova, T. et al. Population development of the invader ctenophore Mnemiopsis leidyi, in the Black Sea and in other seas of the Mediterranean basin. *Mar. Biol.* **139**, 431–445 (2001).
95. Kogovšek, T., Tinta, T., Klun, K. & Malej, A. Jellyfish biochemical composition: importance of standardised sample processing. *Mar. Ecol. Prog. Ser.* **510**, 275–288 (2014).
96. Schrum, C., Alekseeva, I. & St John, M. Development of a coupled physical–biological ecosystem model ECOSMO. *J. Mar. Syst.* **61**, 79–99 (2006).
97. Jakobsen, H. H. & Markager, S. Carbon-to-chlorophyll ratio for phytoplankton in temperate coastal waters: Seasonal patterns and relationship to nutrients: C:Chl for phytoplankton in temperate coastal waters. *Limnol. Oceanogr.* **61**, 1853–1868 (2016).
98. Tilstone, G. H., Land, P. E., Pardo, S., Kerimoglu, O. & Van der Zande, D. Threshold indicators of primary production in the north-east Atlantic for assessing environmental disturbances using 21 years of satellite ocean colour. *Sci. Total Environ.* **854**, 158757 (2023).
99. Fettweis, M. & Van den Eynde, D. The mud deposits and the high turbidity in the Belgian–Dutch coastal zone, southern bight of the North Sea. *Continental Shelf Res.* **23**, 669–691 (2003).
100. Billen, G., Joiris, C., Meyer-Reil, L. & Linderboom, H. Role of bacteria in the North Sea ecosystem. *Neth. J. Sea Res.* **26**, 265–293 (1990).
101. Smyntek, P. M., Teece, M. A., Schulz, K. L. & Thackeray, S. J. A standard protocol for stable isotope analysis of zooplankton in aquatic food web research using mass balance correction models. *Limnol. Oceanogr.* **52**, 2135–2146 (2007).
102. Hentschel, B. T. Intraspecific variations in $\delta^{13}\text{C}$ indicate ontogenetic diet changes in deposit-feeding polychaetes. *Ecology* **79**, 1357–1370 (1998).
103. Jacob, U., Mintenbeck, K., Brey, T., Knust, R. & Beyer, K. Stable isotope food web studies: A case for standardized sample treatment. *Mar. Ecol. Prog. Ser.* **287**, 251–253 (2005).
104. Pinnegar, J. K. & Polunin, N. V. C. Differential fractionation of $\delta^{13}\text{C}$ and $\delta^{15}\text{N}$ among fish tissues: implications for the study of trophic interactions. *Funct. Ecol.* **13**, 225–231 (1999).
105. Oksanen, J. et al. *Vegan: Community Ecology Package*. (2024).
106. De Borger, E. et al. Supplementary information: Offshore wind farms modify coastal food web dynamics by enhancing suspension feeder pathways. *figshare* <https://doi.org/10.6084/m9.figshare.c.7722626.v1> (2025).
107. De Borger, E. edeborger/Foodweb_OWF_publication: v1.0.2 (v1.0.2). *Zenodo*. <https://doi.org/10.5281/zenodo.15042067>. (2025).
108. Verfaillie, E., Van Lancker, V. & Van Meirvenne, M. Multivariate geostatistics for the predictive modelling of the surficial sand distribution in shelf seas. *Continental Shelf Res.* **26**, 2454–2468 (2006).

Acknowledgements

The research leading to the results in this publication was funded through NWO (FOOTPRINT - NWA.1236.18.003) and BELSPO (FaCE-It - Functional biodiversity in a changing sedimentary environment: Implications for biogeochemistry and food webs in a managerial setting - BELSPO - BR/154/A1/FaCE-It; OUTFLOW - Quantifying the contribution of fouling fauna to the local carbon budget of an offshore wind farm - B2/212/P1/OUTFLOW; FED-

tWIN-METRIC - Marine ecosystem responses in a multiple pressures context). We would like to thank the crews of the scientific vessels RV Simon Stevin (VLIZ) and RV Belgica for their assistance during the collection of samples. The research could also not have been completed without the Belgian Scientific Diving Team which is part of the contribution of the Institute of Natural Sciences to EMBRC Belgium. ILVO data on fish and epibenthos densities and biomass were gathered in the framework of several environmental monitoring programmes i.e., the Belgian wind farm monitoring programme (WinMon.BE), sand extraction and dredge disposal monitoring programmes.

Author contributions

Emil De Borger collected field data, conceptualized the food web structure, prepared input scripts and code, analyzed results and wrote the manuscript, Dick van Oevelen worked on model development and analysis and gave manuscript input, Ninon Mavraki collected field-data, performed laboratory analysis and gave manuscript input, Annelies De Backer collected field data and gave manuscript input, Ulrike Braeckman conceptualized the study, collected field-data, and gave manuscript input, Karline Soetaert prepared input scripts and code, gave manuscript input, and supervised the study, Jan vanaverbeke conceptualized the study, collected field-data, gave manuscript input, and supervised the study.

Competing interests

The authors declare no competing interests.

Additional information

Supplementary information The online version contains supplementary material available at <https://doi.org/10.1038/s43247-025-02253-w>.

Correspondence and requests for materials should be addressed to Emil De Borger.

Peer review information *Communications Earth & Environment* thanks Carsten Lemmen and the other, anonymous, reviewer(s) for their contribution to the peer review of this work. Primary Handling Editors: Nadine Schubert, Joe Aslin and Alireza Bahadori. A peer review file is available.

Reprints and permissions information is available at <http://www.nature.com/reprints>

Publisher's note Springer Nature remains neutral with regard to jurisdictional claims in published maps and institutional affiliations.

Open Access This article is licensed under a Creative Commons Attribution-NonCommercial-NoDerivatives 4.0 International License, which permits any non-commercial use, sharing, distribution and reproduction in any medium or format, as long as you give appropriate credit to the original author(s) and the source, provide a link to the Creative Commons licence, and indicate if you modified the licensed material. You do not have permission under this licence to share adapted material derived from this article or parts of it. The images or other third party material in this article are included in the article's Creative Commons licence, unless indicated otherwise in a credit line to the material. If material is not included in the article's Creative Commons licence and your intended use is not permitted by statutory regulation or exceeds the permitted use, you will need to obtain permission directly from the copyright holder. To view a copy of this licence, visit <http://creativecommons.org/licenses/by-nc-nd/4.0/>.

© The Author(s) 2025